Commun. Math. Phys. 291, 403–441 (2009)
Digital Object Identifier (DOI) 10.1007/s00220-009-0769-5

Communications in
Mathematical Physics

On Action-Minimizing Retrograde and Prograde Orbits of the Three-Body Problem

Kuo-Chang Chen, Yu-Chu Lin

Department of Mathematics, National Tsing Hua University, Hsinchu 30013, Taiwan.
E-mail: kchen@math.nthu.edu.tw; d937202@oz.nthu.edu.tw

Received: 13 October 2008 / Accepted: 4 December 2008
Published online: 17 March 2009 – © Springer-Verlag 2009

Abstract: A retrograde orbit of the planar three-body problem is a relative periodic solution with two adjacent masses revolving around each other in one direction while their mass center revolves around the third mass in the other direction. The orbit is said to be prograde or direct if both revolutions follow the same direction. Let $T > 0$ and $\phi \in [0, 2\pi)$ be fixed, and consider the rotating frame which rotates the inertia frame about the origin with angular velocity $\frac{\phi}{T}$. In a recent work of K.-C.Chen [5], the existence of action-minimizing retrograde orbits which are T-periodic on this rotation frame were proved to exist for a large class of masses and a continuum of ϕ. In this paper we generalize the main result in [5], provide some quantitative estimates for admissible masses and mutual distances, and show miscellaneous examples of action-minimizing retrograde orbits. We also show the existence of some prograde and retrograde solutions with additional symmetries.

1. Introduction and Notations

The planar three-body problem concerns the motion of three masses m_1, m_2, m_3 moving in $\mathbb{C}$ in accordance with Newton's law of universal gravitation:

$$m_k \ddot{x}_k = \frac{\partial}{\partial x_k} U(x), \quad k = 1, 2, 3, \tag{1}$$

where $x_k \in \mathbb{C}$ is the position of m_k, $x = (x_1, x_2, x_3)$, and

$$U(x) = \frac{m_1 m_2}{|x_1 - x_2|} + \frac{m_2 m_3}{|x_2 - x_3|} + \frac{m_1 m_3}{|x_1 - x_3|}$$

is the potential energy (negative Newtonian potential). Unless specified otherwise, throughout this paper a "solution" of (1) is referred to a "classical solution" of (1).

A retrograde orbit of the planar three-body problem is a relative periodic solution of (1) with two adjacent masses revolving around each other in one direction while their

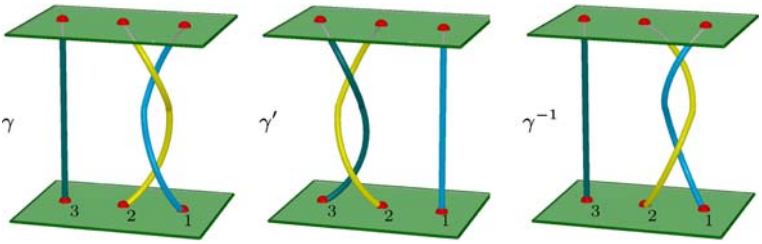

Fig. 1. Retrograde braids γ and γ'

mass center revolves around the third mass in the other direction. The orbit is said to be prograde or direct if both revolutions follow the same direction. By taking an appropriate rotating (synodic) coordinate system and adding a time axis, the trajectory of a relative periodic orbit without collision traces out a pure braid within one period in the three-dimensional space-time. By a pure braid we mean a braid which begins and ends with the same space coordinates. Retrograde and prograde paths can be defined as the collection of collision-free paths which trace out certain braid types in a suitable rotating coordinate system, as illustrated in Fig. 1.

Being retrograde or prograde is a topological property. The idea of using braids to describe topological types of planar periodic solutions is a natural one, see for instance [17,18]. Whether or not a topological class of paths contains a true solution of (1) is in general a difficult task to rigorously verify. The classical lunar theory and analysis of relative equilibria produce numerous solutions that belong to three basic braid types (in an appropriate coordinate frame); namely the prograde, retrograde, and trivial braid types. Among them the prograde and retrograde braids are known to carry solutions for certain masses and for a continuous family of rotating frames. Periodic solutions in other braid classes have not received much rigorous treatment. The figure-8 orbit with equal masses constructed by variational methods provides another example of allowable braid class on both inertia and rotating frames [8,9]. This is a pioneering work which utilizes minimizing methods on the three-body problem and initiates a sequel of research work in the past decade. A vast amount of numerical solutions in various braid classes was recently found for similar choreographic three-body problems [21], some of which may find analytical counterparts in [1,10] but precise determination of topological types for such orbits from equivariant problems and local deformation arguments are yet to be found. Readers are referred to [7,10,14,15,22] for further bibliographies and historical remarks.

The purpose of this paper is to extend the work in [5] which endeavors to prove the existence and minimizing properties of retrograde orbits with various choices of masses. We generalize the main result in [5], provide detailed descriptions and miscellaneous samples of action-minimizing retrograde solutions as well as some prograde and retrograde solutions with additional symmetries. Here we also provide some quantitative estimates for the mutual distances of action-minimizing solutions.

In what follows we provide a more precise and formal definition for retrograde and prograde paths in terms of braids. The definition is slightly more general than the definition in [5]. Fix $\phi \in [0, 2\pi)$ and the relative period $T > 0$, then consider the rotating frame which rotates the inertia frame about the origin with angular velocity ϕ/T. The class of T-periodic loops on this rotating frame is

$$C_{\phi,T} := \{x \in C(\mathbb{R}, \mathbb{C}^3) : x(t+T) = e^{\phi i} x(t) \ \ \forall t \in \mathbb{R}\}.$$

Let $\Delta := \{x \in \mathbb{C}^3 : x_i = x_j \text{ for some } i \neq j\}$ be the variety of collision configurations. The subset

$$C^*_{\phi,T} := \{x \in C_{\phi,T} : x(t) \in \mathbb{C}^3 \setminus \Delta \text{ for any } t \in \mathbb{R}\}$$

of $C_{\phi,T}$ consists of collision-free paths. Each $x = (x_1, x_2, x_3)$ in $C^*_{\phi,T}$ corresponds to a pure braid $\alpha = (\alpha_1, \alpha_2, \alpha_3)$ in $\mathbb{C} \times [0, T]$ with three threads

$$\alpha_k(t) = (e^{\frac{-\phi t}{T} i} x_k(t), t) \in \mathbb{C} \times \mathbb{R},\ t \in [0, T],\ k = 1, 2, 3.$$

This correspondence from $C^*_{\phi,T}$ to the class of pure braids in $\mathbb{C} \times [0, T]$ is clearly bijective.

By relabeling indices if necessary, we may confine our path space to only those which begin and end with collinear configurations and with a prescribed ordering:

$$C^\dagger_{\phi,T} := \{x \in C^*_{\phi,T} : x(0) \in \mathbb{R}^3,\ x_3(0) < x_2(0) < x_1(0)\}.$$

Let $\mathfrak{B} = \mathfrak{B}_{\phi,T}$ be the set of pure braids corresponding to $C^\dagger_{\phi,T}$. Two pure braids in $\mathfrak{B}$ are considered equivalent if one can be continuously deformed to the other among the set $\mathfrak{B}$. Let $\mathbf{R}$ and $\mathbf{R}'$ be the equivalence classes of braids γ and γ' in Fig. 1. *Retrograde paths* in $C^\dagger_{\phi,T}$ are defined as those which have their braids belonging to either $\mathbf{R}$ or $\mathbf{R}'$.

In any two equivalence classes $\mathbf{B}_1$, $\mathbf{B}_2$ of braids we may pick representatives α_1 in $\mathbf{B}_1$, α_2 in $\mathbf{B}_2$ such that $\alpha_1(0) = \alpha_2(0)$. The standard definition of braids multiplication

$$(\alpha_1 \cdot \alpha_2)(t) = \begin{cases} \alpha_1(2t), & t \in [0, T/2] \\ \alpha_2(2t - T), & t \in (T/2, T] \end{cases}$$

induces a well-defined multiplication and group structure for equivalence classes of $\mathfrak{B}$. The multiplicative identity is called the *trivial braid class* belonging to which there is a Euler's relative equilibrium. Paths with braids belonging to inverses $\mathbf{P}$, $\mathbf{P}'$ of braid classes $\mathbf{R}$, $\mathbf{R}'$ are called *prograde paths* (or *direct paths*) in $C_{\phi,T}$. A representative γ^{-1} of $\mathbf{P}$ is depicted in Fig. 1. The concept of retrograde or prograde motion can be defined for some spatial orbits but we shall focus on planar motions in this paper.

In [5] the author proved the existence and minimizing property of retrograde orbits for various choices of masses and for a continuum of $\phi \in (0, \pi]$. In our present work we extend the main result in [5] to a much larger class of masses and wider range of ϕ, see Sects. 2 and 4 for details. Sections 5 and 8 contain miscellaneous examples of action-minimizing orbits. In Sect. 9 we show some quantitative estimates of mutual distances for these orbits. Sections 3, 6, 7 are devoted to proofs of our main theorems.

2. Main Theorems

In this section we state our main theorems on the existence of retrograde orbits for (1) in $C^\dagger_{\phi,T}$, and the existence of retrograde and prograde orbits with additional symmetries. The variational problem described below resembles the one in [5] except that ϕ belongs to $(0, 2\pi)$ instead of $(0, \pi]$. For convenience, and without loss of generality, throughout the rest of this paper we set $T = 1$ and $m_3 = 1$. From now on we drop T from the notations for function spaces and denote $C_{\phi,T}$, $C^*_{\phi,T}$, $C^\dagger_{\phi,T}$, $\mathfrak{B}_{\phi,T}$ respectively by C_ϕ, C^*_ϕ, $C^\dagger_\phi$, $\mathfrak{B}_\phi$.

Let R_ϕ be the set of retrograde paths in $C^\dagger_\phi$ which corresponds to the braid class **R**, a representative of which is the braid γ in Fig. 1. Paths in R_ϕ are initially aligned in the order $x_3(0) < x_2(0) < x_1(0)$, curves x_1 and x_2 revolve clockwise around each other while their center and x_3 revolve counterclockwise around the origin. We may also define R_ϕ as the path component of

$$\left(e^{\phi t i}(1+e^{-2\pi t i}), e^{\phi t i}(1-e^{-2\pi t i}), -e^{\phi t i}\right)$$

in the space $C^\dagger_\phi$.

Each path in C^*_ϕ can be translated to a path with mass center at the origin without altering its braid type; namely, suppose $x \in C^*_\phi$ has mass center $\hat{x} \in C([0,1],\mathbb{C})$, then the new path $(x_1-\hat{x}, x_2-\hat{x}, x_3-\hat{x}) \in C^*_\phi$ and x have the same braid type. Since the center of mass is an integral of motion, it is natural to consider only paths staying inside the *configuration space*

$$V := \{x \in \mathbb{C}^3 : m_1x_1 + m_2x_2 + m_3x_3 = 0\}.$$

Equations (1) are the Euler-Lagrange equations for the *action functional* $\mathcal{A}$: $H^1_{\mathrm{loc}}(\mathbb{R}, V) \to \mathbb{R} \cup \{+\infty\}$ defined by

$$\mathcal{A}(x) := \int_0^1 K(\dot{x}) + U(x)\, dt,$$

where

$$K(\dot{x}) = \frac{1}{2}\left(m_1|\dot{x}_1|^2 + m_2|\dot{x}_2|^2 + m_3|\dot{x}_3|^2\right)$$

is the kinetic energy of the path x. On $H^1_{\mathrm{loc}}(\mathbb{R}, V)$ the action functional $\mathcal{A}$ can be written

$$\mathcal{A}(x) = \frac{1}{M}\sum_{i<j} m_i m_j \int_0^1 \frac{1}{2}|\dot{x}_i - \dot{x}_j|^2 + \frac{M}{|x_i - x_j|}\, dt, \tag{2}$$

where $M = m_1 + m_2 + m_3$ is the total mass.

By choosing a sequence of motionless paths with greater and greater mutual distances, it can be easily seen that the infimum of $\mathcal{A}$ on $H^1_{\mathrm{loc}}(\mathbb{R}, V)$ is zero, which is not attained. To ensure solvability of the action-minimizing problem, we fix $\phi \in (0, 2\pi)$ and consider the following subspace of C_ϕ:

$$H_\phi := \{x \in H^1_{\mathrm{loc}}(\mathbb{R}, V) : x(t+1) = e^{\phi i}x(t)\}.$$

The conventional definition of inner product on the Sobolev space $H^1([0,1], V)$ defines an inner product on H_ϕ as well. It can be verified that collision-free critical points of $\mathcal{A}$ restricted to H_ϕ are indeed classical solutions of (1). Any path x in H_ϕ satisfies

$$\langle x(0), x(1)\rangle \le \max\{0, \cos\phi\}\, |x(0)| \cdot |x(1)|,$$

where $\langle\cdot,\cdot\rangle$ denotes the standard scalar product on $(\mathbb{R}^2)^3$. From this condition, the action functional $\mathcal{A}$ restricted to H_ϕ is coercive (that is, $\mathcal{A}(x) \to \infty$ as $\|x\|_{H^1} \to \infty$, see [3, Prop. 2]) and therefore, by weak lower semicontinuity of $\mathcal{A}$ on H_ϕ and a standard argument in variational calculus, attains its infimum on H_ϕ.

Consider a linear transformation σ on H_ϕ defined by

$$(\sigma \cdot x)(t) := \overline{x(-t)}. \tag{3}$$

It is an order-2 isometry on H_ϕ and, because of the rotational symmetry on H_ϕ, the action functional $\mathcal{A}$ is σ-invariant. By Palais' principle of symmetric criticality [19], any collision-free critical point of $\mathcal{A}$ restricted to the subspace

$$H_\phi^{\langle\sigma\rangle} := \{x \in H_\phi : \sigma \cdot x = x\}$$

of σ-invariant paths is also a critical point of $\mathcal{A}$ on H_ϕ, and hence solves (1).

Detailed descriptions and the variational principles mentioned in the above three paragraphs can be found in [3–5].

In order to simplify the statements of our theorems, we define the following auxiliary functions: $J : [0, 1) \to \mathbb{R}_+$, $\xi : \mathbb{R}_+^2 \times (0, 2) \to \mathbb{R}$, and $E : \mathbb{R}_+^2 \to (1, 2)$ by

$$J(s) := \int_0^1 \frac{1}{|1 - s\, e^{2\pi t i}|}\, dt, \tag{4}$$

$$\xi(m_1, m_2, \eta) := \frac{1}{(m_1 + m_2 + 1)^{\frac{1}{3}}(m_1 + m_2)^{\frac{2}{3}}} \left(\frac{\eta}{2 - \eta}\right)^{\frac{2}{3}}, \tag{5}$$

$$E(m_1, m_2) := \frac{2\sqrt{m_1 + m_2 + 1}\,(m_1 + m_2)}{\sqrt{m_1 + m_2 + 1}\,(m_1 + m_2) + \max\{m_1, m_2\}^{\frac{3}{2}}}. \tag{6}$$

Theorem 1. *Given $\phi = \eta\pi$, $\eta \in (0, 2)$. Let $m_3 = 1$ and let J, $\xi = \xi(m_1, m_2, \eta)$, E be as in (4), (5), (6). Suppose*

$$\eta < E(m_1, m_2), \tag{7}$$

$$\eta^{\frac{2}{3}} \left\{ \tfrac{m_1 m_2}{(m_1+m_2)\xi} + \tfrac{2}{3} \left[m_1 \left(J\left(m_2 \xi\right) - 1 \right) + m_2 \left(J\left(m_1 \xi\right) - 1 \right) \right] \right\} < (2 - \eta)^{\frac{2}{3}} m_1 m_2 + \min\left\{ (2^{\frac{2}{3}} - (2 - \eta)^{\frac{2}{3}}) m_1 m_2,\ (2^{\frac{2}{3}} - \eta^{\frac{2}{3}}) m_1,\ (2^{\frac{2}{3}} - \eta^{\frac{2}{3}}) m_2 \right\}. \tag{8}$$

Then the three-body problem (1) has a retrograde solution in $C_\phi^\dagger$ which minimizes the action functional $\mathcal{A}$ in $R_\phi \cap H_\phi^{\langle\sigma\rangle}$.

Theorem 1 provides a criterion on the masses (m_1, m_2) with which an action-minimizing retrograde solution in $C_\phi^\dagger$ for (1) exists. Solutions obtained by Theorem 1 are periodic if ϕ/π is rational and are quasi-periodic if ϕ/π is irrational. The condition (7) is fulfilled for all $\eta \in (0, 1]$ and for some $\eta \in (1, 2)$, depending on the values of m_1 and m_2. The condition (8) is also valid for a wide range of (m_1, m_2) when $\eta \in (0, 1]$. Roughly speaking, straightforward calculations show that the first term in the first line of (8) is significantly dominated by the terms in the second line for most choices of masses, and the remaining terms in the first line are generally very small since $J(s)$ is fairly close to 1 for most $s \in (0, 1)$ (see the appendix of [5]).

We will see in Sect. 4 that the assumptions (7) and (8) in Theorem 1 are much less restrictive than the conditions imposed to the main result in [5]. When $\eta \in (0, 1]$, Proposition 5 in Sect. 4 provides a precise and simple criterion for (m_1, m_2) to satisfy the requirements of Theorem 1, and the theorem tells us that "most" choices of masses

are admissible regardless of the value of $\eta \in (0, 1]$. Many numerical figures for these retrograde action minimizers will be presented in Sect. 5.

In addition to the isometry σ given in (3), consider the linear transformation τ on H_ϕ defined by

$$(\tau \cdot x)(t) := e^{-\frac{\phi}{2}i}(x_2, x_1, x_3)\left(t + \frac{T}{2}\right). \tag{9}$$

It is another order-2 isometry on H_ϕ. The action functional $\mathcal{A}$ is τ-invariant provided $m_1 = m_2 = m$. Let $\langle \sigma, \tau \rangle$ be the group of isometries on H_ϕ generated by σ and τ. Following again from Palais' principle of symmetric criticality, any collision-free critical point of $\mathcal{A}$ restricted to the subspace

$$H_\phi^{\langle \sigma, \tau \rangle} := \{x \in H_\phi : g \cdot x = x \ \text{ for any } g \in \langle \sigma, \tau \rangle\}$$

of $\langle \sigma, \tau \rangle$-invariant paths is also a critical point of $\mathcal{A}$ on H_ϕ, and hence solves (1).

Theorem 2. *Given $\phi = \eta\pi$, $\eta \in (0, 2)$. Let J, ξ be as in (4), (5) with $m_3 = 1$ and $m_1 = m_2 = m$. Suppose*

$$\eta < \frac{4\sqrt{2m+1}}{2\sqrt{2m+1}+\sqrt{m}}, \tag{10}$$

$$\eta^{\frac{2}{3}}\left[\tfrac{1}{3} + \tfrac{1}{4\xi} + \tfrac{2}{3}J(m\xi)\right] < \min\left\{2^{\frac{1}{3}}m + \eta^{\frac{2}{3}},\ \tfrac{m}{2}(2-\eta)^{\frac{2}{3}} + 2^{\frac{2}{3}}\right\}. \tag{11}$$

Then the three-body problem (1) has a retrograde solution in $C_\phi^\dagger$ which minimizes the action functional $\mathcal{A}$ in $R_\phi \cap H_\phi^{\langle \sigma, \tau \rangle}$.

The region of (m, η) which satisfies (11) extends the regions of admissible masses given in Theorem 1. In particular, for fixed (m_1, m_2) the inequality (8) fails to hold if η is sufficiently small, but (11) holds for arbitrarily small η as long as m is not close to zero. Section 5 includes several numerical figures of the action-minimizing retrograde solutions obtained by Theorem 2, and Sect. 8 shows the region of admissible (m, η). The special case $m_1 = m_2 = m_3 = 1$ includes part of the retrograde revolution family discovered numerically by Broucke [2] and Hénon [12].

Let P_ϕ be the set of prograde paths in $C_\phi^\dagger$ corresponding to the braid class $\mathbf{P}$, the multiplicative inverse of $\mathbf{R}$ in $\mathfrak{B}$. Paths in P_ϕ are initially aligned in the order $x_3(0) < x_2(0) < x_1(0)$, curves x_1 and x_2 revolve counterclockwise around each other while their center and x_3 revolve counterclockwise around the origin. We may also define P_ϕ as the path component of

$$\left(e^{\phi t i}(1 + e^{2\pi t i}),\ e^{\phi t i}(1 - e^{2\pi t i}),\ -e^{\phi t i}\right)$$

in the space $C_\phi^\dagger$.

Consider another auxiliary function $\zeta : \mathbb{R}_+^2 \times (0, 2) \to \mathbb{R}$ defined by

$$\zeta(m, \eta) := \frac{1}{(2m+1)^{\frac{1}{3}}(2m)^{\frac{2}{3}}}\left(\frac{\eta}{2+\eta}\right)^{\frac{2}{3}}. \tag{12}$$

Theorem 3. *Given $\phi = \eta\pi$, $\eta \in (0, 2)$. Let $m_3 = 1$, $m_1 = m_2 = m$, and J, $\zeta = \zeta(m, \eta)$ be as in (4), (12). Suppose*

$$\eta^{\frac{2}{3}} \left[\frac{1}{3} + \frac{1}{4\zeta} + \frac{2}{3} J(m\zeta) \right] < \min \left\{ 2^{\frac{1}{3}} m + \eta^{\frac{2}{3}},\ \frac{m}{2}(2+\eta)^{\frac{2}{3}} + 2^{\frac{2}{3}} \right\}. \tag{13}$$

Then the three-body problem (1) has a prograde solution in $C^{\dagger}_{\phi}$ which minimizes the action functional $\mathcal{A}$ in $P_\phi \cap H^{\langle \sigma, \tau \rangle}_{\phi}$.

In Sect. 8 we show the region of (m, η) which satisfies (13) and several numerical figures for the action-minimizing prograde orbits obtained by Theorem 3. The special case $m_1 = m_2 = m_3 = 1$ includes part of the direct revolution family in [2].

3. Proof of Theorem 1

The proof presented here is an improvement of the proof for the main result in [5, Theorem 5], where some estimates are refined here and the rotation angle $\phi \in (0, \pi]$ is extended to $\phi = \eta\pi \in (0, 2\pi)$. The lower bound estimate for action values over collision paths in [5] is derived based on the symmetry constraint. Here we refine the estimates by taking both the symmetry and topological constraints into consideration. The improvement is significant especially when ϕ is away from π.

As observed earlier, the action functional $\mathcal{A}$ is coercive on H_ϕ and therefore it attains its infimum on every weakly closed subset of H_ϕ. In particular, it attains its infimum on the weak closure of $R_\phi \cap H^{\langle \sigma \rangle}_{\phi}$ at some z_ϕ. Furthermore, as mentioned in the previous section, collision-free critical points of $\mathcal{A}$ on $H^{\langle \sigma \rangle}_{\phi}$ are solutions to (1), If z_ϕ is collision-free, then it certainly solves (1) since $R_\phi \cap H^{\langle \sigma \rangle}_{\phi}$ is relatively open in $H^{\langle \sigma \rangle}_{\phi}$.

To prove Theorem 1, it is sufficient to prove that z_ϕ does not belong to the weak boundary $\partial R_\phi \cap H^{\langle \sigma \rangle}_{\phi}$ of $R_\phi \cap H^{\langle \sigma \rangle}_{\phi}$ under the assumptions (7), (8). What we will prove is the inequality

$$\inf_{x \in R_\phi \cap H^{\langle \sigma \rangle}_{\phi}} \mathcal{A}(x) < \inf_{x \in \partial R_\phi \cap H^{\langle \sigma \rangle}_{\phi}} \mathcal{A}(x) \tag{14}$$

under the given conditions on ϕ and masses. This will be accomplished by providing good estimates for both sides of (14).

A good lower bound estimate for the right side of (14) can be obtained by using a key formula in [5], which is motivated by Gordon's theorem [11], and which we describe in Proposition 4 below.

Given any $\theta \in (0, \pi]$, $T > 0$, consider the following path space:

$$\Gamma_{T,\theta} := \{\mathbf{r} \in H^1([0, T], \mathbb{C}) :\ \langle \mathbf{r}(0), \mathbf{r}(T) \rangle = |\mathbf{r}(0)||\mathbf{r}(T)| \cos\theta\},$$
$$\Gamma^*_{T,\theta} := \{\mathbf{r} \in \Gamma_{T,\theta} :\ \mathbf{r}(t) = 0 \ \text{ for some } t \in [0, T]\}.$$

The symbol $\langle \cdot, \cdot \rangle$ stands for the standard scalar product in $\mathbb{R}^2 \cong \mathbb{C}$. Define the Keplerian action functional $I_{\mu,\alpha,T} : H^1([0, T], \mathbb{C}) \to \mathbb{R} \cup \{+\infty\}$ by

$$I_{\mu,\alpha,T}(\mathbf{r}) := \int_0^T \frac{\mu}{2} |\dot{\mathbf{r}}|^2 + \frac{\alpha}{|\mathbf{r}|}\, dt.$$

Proposition 4. *Let $\theta \in (0, \pi]$, $T > 0$, $\mu > 0$, $\alpha > 0$ be constants. Then*

$$\inf_{\mathbf{r}\in\Gamma_{T,\theta}} I_{\mu,\alpha,T}(\mathbf{r}) = \frac{3}{2}(\mu\alpha^2\theta^2 T)^{\frac{1}{3}}, \tag{15}$$

$$\inf_{\mathbf{r}\in\Gamma^*_{T,\theta}} I_{\mu,\alpha,T}(\mathbf{r}) = \frac{3}{2}(\mu\alpha^2\pi^2 T)^{\frac{1}{3}}. \tag{16}$$

Given $x \in R_\phi \cap H_\phi^{\langle\sigma\rangle}$, according to σ-invariance and the definition of H_ϕ, all masses are aligned on the real axis at $t = 0$, and

$$e^{-\frac{\phi}{2}i}x(t) \;=\; e^{-\frac{\phi}{2}i}\overline{x(-t)} \;=\; \overline{e^{\frac{\phi}{2}i}x(-t)} \;=\; \overline{e^{-\frac{\phi}{2}i}x(1-t)}. \tag{17}$$

This tells us that $x(t)$ and $x(1-t)$ are symmetric with respect to the line $L_{\frac{\phi}{2}} = \{re^{\frac{\phi}{2}i} : r \in \mathbb{R}\}$ and, in particular, all masses are aligned on $L_{\frac{\phi}{2}}$ when $t = \frac{1}{2}$. Furthermore,

$$I_{1,M,1}(x_i - x_j) = 2I_{1,M,\frac{1}{2}}(x_i - x_j) \tag{18}$$

for each pair of i, j. Here $M = m_1 + m_2 + 1$ is the total mass.

Suppose $x \in \partial R_\phi$, then $x_i(t) = x_j(t)$ for some $t \in [0, \frac{1}{2}]$ and $i \neq j$. Assume for now $i = 1$, $j = 2$. Then

$$x_1 - x_2 \in \Gamma^*_{\frac{1}{2},\frac{\phi}{2}} \text{ or } \Gamma^*_{\frac{1}{2},\pi-\frac{\phi}{2}},$$
$$x_1 - x_3,\ x_2 - x_3 \in \Gamma_{\frac{1}{2},\frac{\phi}{2}} \text{ or } \Gamma_{\frac{1}{2},\pi-\frac{\phi}{2}}.$$

If $x_1 - x_3$ belongs to $\Gamma_{\frac{1}{2},\frac{\phi}{2}}$, then by Proposition 4 we have

$$I_{1,M,\frac{1}{2}}(x_1 - x_3) \;\geq\; \frac{3}{2}\left(\frac{M\phi}{2}\right)^{\frac{2}{3}}\left(\frac{1}{2}\right)^{\frac{1}{3}} \;=\; \frac{3}{4}M^{\frac{2}{3}}\phi^{\frac{2}{3}}.$$

If $x_1 - x_3$ belongs to $\Gamma_{\frac{1}{2},\pi-\frac{\phi}{2}}$, we claim that x_1 and x_3 actually collide on $[0, \frac{1}{2}]$, thus

$$x_1 - x_3 \in \Gamma^*_{\frac{1}{2},\pi-\frac{\phi}{2}}.$$

Suppose not, then $x_1(t) - x_3(t) \neq 0$ for every $t \in [0, \frac{1}{2}]$, implying that $x_1(t) - x_3(t) \neq 0$ for all t. All paths in a small C^0-neighborhood of x would have the same value of $Deg(x_1 - x_3)$, the degree of $x_1(t) - x_3(t)$ over $[0, 1]$ on the rotating frame. The reflection symmetry (17) plus the condition $x_1 - x_3 \in \Gamma_{\frac{1}{2},\pi-\frac{\phi}{2}}$ force $x_1 - x_3$ to have nonzero winding number about the origin on the rotating frame over the time interval $[0, 1]$. This contradicts the assumption that $x \in \partial R_\phi$, because any path y in R_ϕ must satisfy $Deg(y_1 - y_3) = 0$, and the weak limit (which is also the uniform limit) x of any sequence $y^{(n)}$ in R_ϕ must either have $Deg(x_1 - x_3) = 0$ or $x_1(t) - x_3(t) = 0$ for some t. Now, knowing that $x_1(t) - x_3(t) = 0$ for some $t \in [0, \frac{1}{2}]$, by Proposition 4 we obtain a larger lower bound estimate for $I_{1,M,\frac{1}{2}}(x_1 - x_3)$:

$$I_{1,M,\frac{1}{2}}(x_1 - x_3) \;\geq\; \frac{3}{2}(M\pi)^{\frac{2}{3}}\left(\frac{1}{2}\right)^{\frac{1}{3}}.$$

The same arguments and estimates hold for $I_{1,M,\frac{1}{2}}(x_2 - x_3)$.

By (2), (15), (16), and (17),

$$\begin{aligned}
\mathcal{A}(x) &= \tfrac{2}{M} \textstyle\sum_{i<j} m_i m_j \int_0^{\frac{1}{2}} \tfrac{1}{2}|\dot{x}_i - \dot{x}_j|^2 + \tfrac{M}{|x_i - x_j|}\, dt \\
&= \tfrac{2}{M}\left[m_1 m_2\, I_{1,M,\frac{1}{2}}(x_1 - x_2) + m_1 m_3\, I_{1,M,\frac{1}{2}}(x_1 - x_3) + m_2 m_3\, I_{1,M,\frac{1}{2}}(x_2 - x_3)\right] \\
&\geq \tfrac{2}{M}\left[\tfrac{3}{2} m_1 m_2 M^{\frac{2}{3}} \pi^{\frac{2}{3}} \left(\tfrac{1}{2}\right)^{\frac{1}{3}} + \tfrac{3}{4}(m_1 m_3 + m_2 m_3) M^{\frac{2}{3}} \phi^{\frac{2}{3}}\right] \\
&= \tfrac{3}{2}\left(\tfrac{\pi^2}{M}\right)^{\frac{1}{3}} \left[2^{\frac{2}{3}} m_1 m_2 + \eta^{\frac{2}{3}}(m_1 m_3 + m_2 m_3)\right].
\end{aligned}$$

Now we consider the second case: $x_1(t) = x_3(t)$ for some $t \in [0, \frac{1}{2}]$. Then, as in the previous case,

$$\begin{aligned}
x_1 - x_3 &\in \Gamma^*_{\frac{1}{2},\frac{\phi}{2}} \text{ or } \Gamma^*_{\frac{1}{2},\pi-\frac{\phi}{2}}, \\
x_1 - x_2,\ x_2 - x_3 &\in \Gamma_{\frac{1}{2},\frac{\phi}{2}} \text{ or } \Gamma_{\frac{1}{2},\pi-\frac{\phi}{2}}.
\end{aligned}$$

If $x_2 - x_3$ belongs to $\Gamma_{\frac{1}{2},\frac{\phi}{2}}$, then by Proposition 4 we have

$$I_{1,M,\frac{1}{2}}(x_2 - x_3) \;\geq\; \frac{3}{2}\left(\frac{M\phi}{2}\right)^{\frac{2}{3}} \left(\frac{1}{2}\right)^{\frac{1}{3}} \;=\; \frac{3}{4} M^{\frac{2}{3}} \phi^{\frac{2}{3}}.$$

If $x_2 - x_3$ belongs to $\Gamma_{\frac{1}{2},\pi-\frac{\phi}{2}}$, then following the arguments above, x_2 and x_3 actually collide on $[0, \frac{1}{2}]$, and thus

$$\begin{aligned}
x_2 - x_3 &\in \Gamma^*_{\frac{1}{2},\pi-\frac{\phi}{2}}, \\
I_{1,M,\frac{1}{2}}(x_2 - x_3) &\geq \frac{3}{2}(M\pi)^{\frac{2}{3}} \left(\frac{1}{2}\right)^{\frac{1}{3}} \left(\geq \frac{3}{4} M^{\frac{2}{3}} \phi^{\frac{2}{3}}\right).
\end{aligned}$$

If $x_1 - x_2$ belongs to $\Gamma_{\frac{1}{2},\pi-\frac{\phi}{2}}$, then by Proposition 4 we have

$$I_{1,M,\frac{1}{2}}(x_1 - x_2) \;\geq\; \frac{3}{2}\left(\frac{M(2\pi - \phi)}{2}\right)^{\frac{2}{3}} \left(\frac{1}{2}\right)^{\frac{1}{3}} \;=\; \frac{3}{4} M^{\frac{2}{3}} (2\pi - \phi)^{\frac{2}{3}}.$$

If $x_1 - x_2$ belongs to $\Gamma_{\frac{1}{2},\frac{\phi}{2}}$, then x_1 and x_2 must collide on $[0, \frac{1}{2}]$, because otherwise the reflection symmetry (17) plus the condition $x_1 - x_2 \in \Gamma_{\frac{1}{2},\frac{\phi}{2}}$ force $x_1 - x_2$ to have an even winding number about the origin over the time interval $[0, 1]$, contradicting the assumption that $x \in \partial R_\phi$. In this case we have

$$x_1 - x_2 \in \Gamma^*_{\frac{1}{2},\frac{\phi}{2}},$$

and therefore

$$I_{1,M,\frac{1}{2}}(x_1 - x_2) \;\geq\; \frac{3}{2}(M\pi)^{\frac{2}{3}} \left(\frac{1}{2}\right)^{\frac{1}{3}} \left(\geq \frac{3}{4} M^{\frac{2}{3}} (2\pi - \phi)^{\frac{2}{3}}\right).$$

As in the previous case, by (2), (15), (16), and (17),

$$\begin{aligned}
&\mathcal{A}(x)\\
&= \frac{2}{M}\left[m_1m_2\, I_{1,M,\frac{1}{2}}(x_1-x_2) + m_1m_3\, I_{1,M,\frac{1}{2}}(x_1-x_3) + m_2m_3\, I_{1,M,\frac{1}{2}}(x_2-x_3)\right]\\
&\geq \frac{2}{M}\left[\frac{3}{4}m_1m_2M^{\frac{2}{3}}(2\pi-\phi)^{\frac{2}{3}} + \frac{3}{2}m_1m_3M^{\frac{2}{3}}\pi^{\frac{2}{3}}\left(\frac{1}{2}\right)^{\frac{1}{3}} + \frac{3}{4}m_2m_3M^{\frac{2}{3}}\phi^{\frac{2}{3}}\right]\\
&= \frac{3}{2}\left(\frac{\pi^2}{M}\right)^{\frac{1}{3}}\left[(2-\eta)^{\frac{2}{3}}m_1m_2 + 2^{\frac{2}{3}}m_1m_3 + \eta^{\frac{2}{3}}m_2m_3\right].
\end{aligned}$$

The third case, $x_2(t) = x_3(t)$ for some $t \in [0, \frac{1}{2}]$, is similar to the second case. In this case we have

$$\begin{aligned}
&\mathcal{A}(x)\\
&\geq \frac{2}{M}\left[\frac{3}{4}m_1m_2M^{\frac{2}{3}}(2\pi-\phi)^{\frac{2}{3}} + \frac{3}{4}m_1m_3M^{\frac{2}{3}}\phi^{\frac{2}{3}} + \frac{3}{2}m_2m_3M^{\frac{2}{3}}\pi^{\frac{2}{3}}\left(\frac{1}{2}\right)^{\frac{1}{3}}\right]\\
&= \frac{3}{2}\left(\frac{\pi^2}{M}\right)^{\frac{1}{3}}\left[(2-\eta)^{\frac{2}{3}}m_1m_2 + \eta^{\frac{2}{3}}m_1m_3 + 2^{\frac{2}{3}}m_2m_3\right].
\end{aligned}$$

Summarizing the above estimates, and by setting $m_3 = 1$, we conclude that

$$\begin{aligned}
&\inf_{x\in\partial R_\phi\cap H_\phi^{\langle\sigma\rangle}} \mathcal{A}(x)\\
&\geq \frac{3}{2}\left(\frac{\pi^2}{M}\right)^{\frac{1}{3}} \min\left\{2^{\frac{2}{3}}m_1m_2 + \eta^{\frac{2}{3}}(m_1+m_2), (2-\eta)^{\frac{2}{3}}m_1m_2 + 2^{\frac{2}{3}}m_1 + \eta^{\frac{2}{3}}m_2,\right.\\
&\quad \left.(2-\eta)^{\frac{2}{3}}m_1m_2 + \eta^{\frac{2}{3}}m_1 + 2^{\frac{2}{3}}m_2\right\}\\
&= \frac{3}{2}\left(\frac{\pi^2}{M}\right)^{\frac{1}{3}}\left[(2-\eta)^{\frac{2}{3}}m_1m_2 + \eta^{\frac{2}{3}}(m_1+m_2)\right.\\
&\quad \left.+\min\left\{(2^{\frac{2}{3}} - (2-\eta)^{\frac{2}{3}})m_1m_2, (2^{\frac{2}{3}} - \eta^{\frac{2}{3}})m_1, (2^{\frac{2}{3}} - \eta^{\frac{2}{3}})m_2\right\}\right]. \qquad (19)
\end{aligned}$$

This provides a lower bound estimate for the right side of (14).

Now we look for a good upper bound estimate for the left side of (14). Let

$$\begin{aligned}
Q(t) &:= \frac{1}{(M\phi)^{\frac{2}{3}}}e^{\phi ti},\\
R(t) &:= \frac{1}{(m_1+m_2)^{\frac{2}{3}}(2\pi-\phi)^{\frac{2}{3}}}e^{(\phi-2\pi)ti},
\end{aligned}$$

and consider an artificial path

$$\begin{aligned}
x^{(\phi)}(t) &= (x_1^{(\phi)}(t), x_2^{(\phi)}(t), x_3^{(\phi)}(t))\\
&:= (Q(t) + m_2R(t),\ Q(t) - m_1R(t),\ -(m_1+m_2)\,Q(t)). \qquad (20)
\end{aligned}$$

Then $x^{(\phi)}$ has the initial ordering as required in the definition of $C_\phi^\dagger$. Particles $x_1^{(\phi)}$ and $x_2^{(\phi)}$ revolve clockwise about their mass center $Q(t)$ along circular paths, while $Q(t)$ and $x_3^{(\phi)}$ revolve counterclockwise along circular paths about the origin, which is exactly the mass center of $x^{(\phi)}$. Clearly $x^{(\phi)}$ belongs to $H_\phi^{\langle\sigma\rangle}$. The assumption (7) is equivalent to

$$\frac{\max\{m_1,m_2\}^{\frac{3}{2}}}{\sqrt{M}(m_1+m_2)} \;<\; \frac{2-\eta}{\eta} \;=\; \frac{2\pi-\phi}{\phi},$$

or

$$\max\{m_1,m_2\}|R(t)| \;=\; \frac{\max\{m_1,m_2\}}{(m_1+m_2)^{\frac{2}{3}}(2\pi-\phi)^{\frac{2}{3}}} \;<\; \left(\frac{M}{\phi^2}\right)^{\frac{1}{3}} \;=\; M|Q(t)|.$$

This inequality is equivalent to the condition that the circular path $x_3^{(\phi)}$ never touch the line segment connecting $x_1^{(\phi)}$ and $x_2^{(\phi)}$. From this observation we see that $x^{(\phi)}$ belongs to $R_\phi \cap H_\phi^{\langle\sigma\rangle}$ if and only if (7) holds.

Straightforward calculations show that

$$|\dot{x}_1^{(\phi)}|^2 = \left(\frac{\phi}{M^2}\right)^{\frac{2}{3}} + m_2^2\frac{(2\pi-\phi)^{\frac{2}{3}}}{(m_1+m_2)^{\frac{4}{3}}} - 2m_2\frac{\phi^{\frac{1}{3}}(2\pi-\phi)^{\frac{1}{3}}}{M^{\frac{2}{3}}(m_1+m_2)^{\frac{2}{3}}}\cos(2\pi t),$$

$$|\dot{x}_2^{(\phi)}|^2 = \left(\frac{\phi}{M^2}\right)^{\frac{2}{3}} + m_1^2\frac{(2\pi-\phi)^{\frac{2}{3}}}{(m_1+m_2)^{\frac{4}{3}}} + 2m_1\frac{\phi^{\frac{1}{3}}(2\pi-\phi)^{\frac{1}{3}}}{M^{\frac{2}{3}}(m_1+m_2)^{\frac{2}{3}}}\cos(2\pi t),$$

$$|\dot{x}_3^{(\phi)}|^2 = (m_1+m_2)^2\left(\frac{\phi}{M^2}\right)^{\frac{2}{3}},$$

$$K(\dot{x}^{(\phi)}) = \frac{1}{2}\left[(m_1+m_2)\left(\frac{\phi^2}{M}\right)^{\frac{1}{3}} + \frac{m_1m_2(2\pi-\phi)^{\frac{2}{3}}}{(m_1+m_2)^{\frac{1}{3}}}\right].$$

Note that the last line is independent of time. It can be easily verified that (7) ensures both $m_1\xi$ and $m_2\xi$ are strictly less than 1. The contribution of $U(x^{(\phi)})$ to the total action can therefore be written

$$\begin{aligned}
&\int_0^1 U(x^{(\phi)})\,dt\\
&= \int_0^1 \frac{m_1m_2}{|x_1^{(\phi)}-x_2^{(\phi)}|} + \frac{m_1}{|x_1^{(\phi)}-x_3^{(\phi)}|} + \frac{m_2}{|x_2^{(\phi)}-x_3^{(\phi)}|}\,dt\\
&= \int_0^1 \frac{m_1m_2(2\pi-\phi)^{\frac{2}{3}}}{(m_1+m_2)^{\frac{1}{3}}} + \left(\frac{\phi^2}{M}\right)^{\frac{1}{3}}\frac{m_1}{|1-m_2\xi e^{-2\pi ti}|} + \left(\frac{\phi^2}{M}\right)^{\frac{1}{3}}\frac{m_2}{|1-m_1\xi e^{-2\pi ti}|}\,dt\\
&= \frac{m_1m_2(2\pi-\phi)^{\frac{2}{3}}}{(m_1+m_2)^{\frac{1}{3}}} + \left(\frac{\phi^2}{M}\right)^{\frac{1}{3}}\left(m_1J(m_2\xi)+m_2J(m_1\xi)\right).
\end{aligned}$$

Here $\xi = \xi(m_1,m_2,\eta)$ is as in (5). Therefore,

$$\begin{aligned}
&\inf_{x\in R_\phi\cap H_\phi^{\langle\sigma\rangle}}\mathcal{A}(x) \le \frac{3m_1m_2(2\pi-\phi)^{\frac{2}{3}}}{2(m_1+m_2)^{\frac{1}{3}}} + \left(\frac{\phi^2}{M}\right)^{\frac{1}{3}}\left[\frac{m_1+m_2}{2} + m_1J(m_2\xi)+m_2J(m_1\xi)\right]\\
&= \left(\frac{\eta^2\pi^2}{M}\right)^{\frac{1}{3}}\left[\frac{3m_1m_2}{2(m_1+m_2)\xi} + \frac{3(m_1+m_2)}{2} + m_1\left(J(m_2\xi)-1\right) + m_2\left(J(m_1\xi)-1\right)\right]. \quad (21)
\end{aligned}$$

The assumption (8) is easily seen to be equivalent to that the upper bound estimate in (21) is strictly less than the lower bound estimate in (19). Therefore (8) implies our desired inequality (14). This completes the proof for Theorem 1.

4. Region of Admissible Masses

The region of admissible (m_1, m_2) given by Theorem 1 depends on the choice of $\phi = \eta\pi \in (0, 2\pi)$. The values of the function

$$E(m_1, m_2) = \frac{2\sqrt{M}(m_1 + m_2)}{\sqrt{M}(m_1 + m_2) + \max\{m_1, m_2\}^{\frac{3}{2}}}$$

are strictly between 1 and 2. The region of (m_1, m_2) satisfying (7) shrinks rapidly as the angle ϕ approaches 2π. In fact, when ϕ is close to 2π the braid type of the path $x^{(\phi)}$ given in the previous section is the same as the Euler relative equilibrium E_3 which rotates with angular velocity $\pi - \phi$ and which begins with ordering $x_2(0) < x_3(0) < x_1(0)$.

Figure 2 shows the regions of admissible masses determined by (8) with various ϕ, which increases from 0.01π to 1.35π. The condition (7) is automatic when $\phi \in (0, \pi]$. When $\phi \in (\pi, 2\pi)$, the diagonal component of the region is the region of admissible masses which satisfy both (7) and (8). This component is unbounded when $\phi \in (0, \pi]$ and it rapidly shrinks to a bounded region as ϕ increases until the region diminishes when $\phi \approx 1.38\pi$. The two triangular regions which border coordinate axes with $\phi \geq 1.2$ are regions where (8) holds but (7) fails.

The next proposition states that for any $\phi \in (0, \pi]$, "most" choices of masses are admissible. What we mean here is that, if a pair of positive masses (m_1, m_2) are randomly chosen from a large ball on the m_1m_2-mass plane, the odds that they fall inside the region of admissible masses is more than 0.5. For this purpose it is sufficient to show that (8) is fulfilled whenever

$$\frac{2}{5} \leq \frac{m_1}{m_2} \leq \frac{5}{2}$$

except possibly a bounded region in the m_1m_2-mass plane. One can easily verify that the proportion of (m_1, m_2) in region $\{m_1, m_2 \geq 0, m_1^2 + m_2^2 \leq R^2\}$ satisfying the above inequalities is approximately 51.55% when R is sufficiently large. In Proposition 5 we replace the ratio bound $5/2$ by 3, which allows us to improve the odds of choosing "good" masses from at least 51.55% to at least 59.03%, regardless of the value of $\phi \in (0, \pi]$. This is far from optimal and significantly better bounds can be found when the estimates are carried out for individual values of ϕ. For example, in [5, Example 6] the ratio m_1/m_2 is bounded by $1/6$ and 6 when $\phi = \pi$, and the coverage of admissible masses satisfying these specific bounds is approximately 78.97%.

Proposition 5. *For any $\phi = \eta\pi \in (0, \pi]$, the inequality (8) holds whenever*

$$m_1, m_2 \geq \overline{m} := \frac{2^{\frac{2}{3}} - \eta^{\frac{2}{3}}}{2^{\frac{2}{3}} - (2 - \eta)^{\frac{2}{3}}} \text{ and } \frac{1}{3} \leq \frac{m_1}{m_2} \leq 3.$$

Proof. The inequality (8) is unchanged by swapping m_1 and m_2, thus we only need to show that (8) holds whenever $\overline{m} \leq m_1 \leq m_2 \leq 3m_1$.

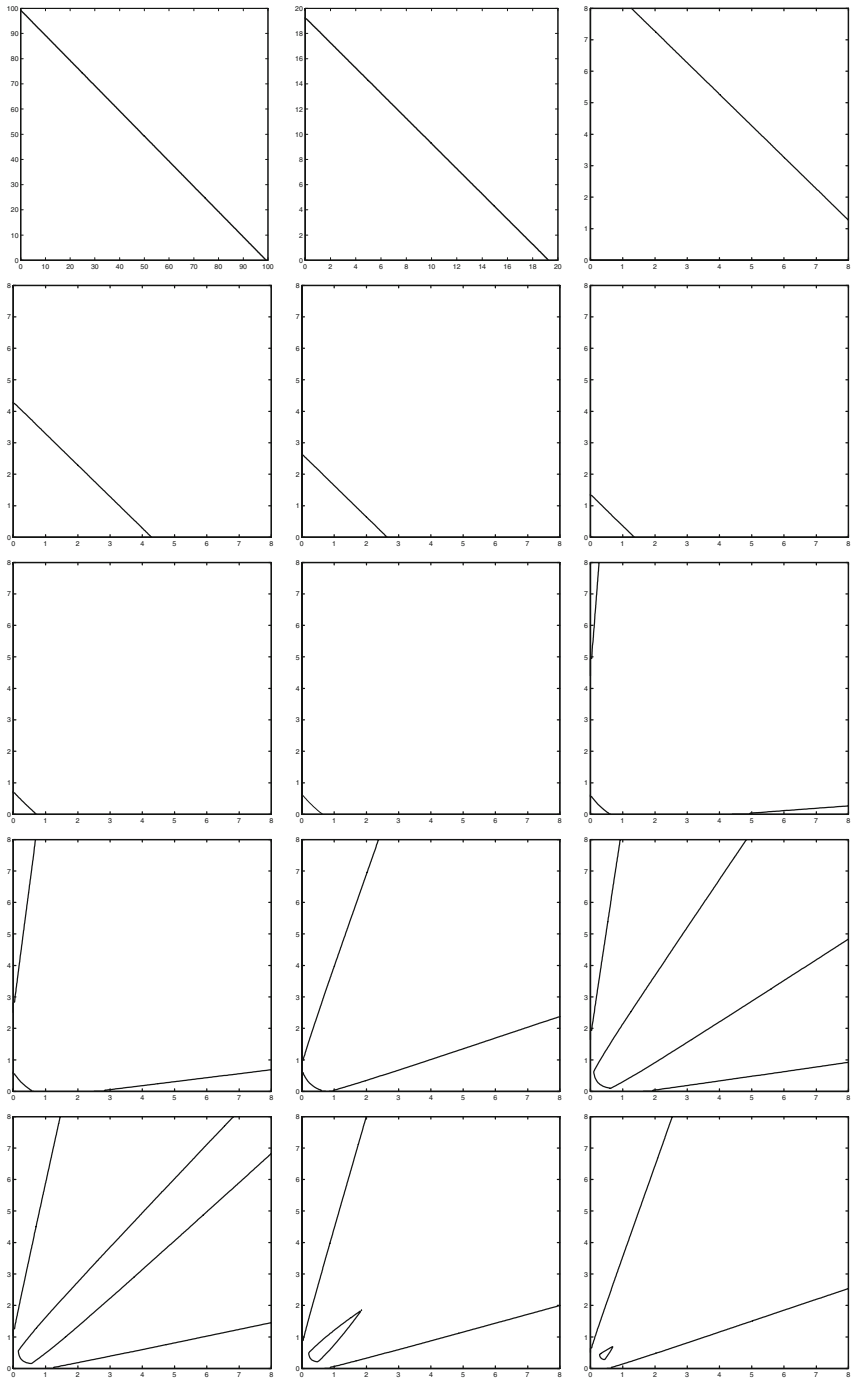

Fig. 2. Regions of admissible masses with ϕ equal (from top left to the bottom right) 0.01π, 0.05π, 0.1π, 0.2π, 0.3π, 0.5π, 0.8π, 0.9π, 0.97π, π, 1.1π, 1.2π, 1.25π, 1.3π, 1.35π. The mass region for the first figure is $0 < m_1, m_2 \leq 100$, the second one is $0 < m_1, m_2 \leq 20$, others are $0 < m_1, m_2 \leq 8$

Let $m_1 = m, m_2 = \lambda m$. Then $\lambda \in [1, 3]$, $\eta = \phi/\pi \in (0, 1]$, and

$$\xi(m, \lambda m, \eta) = \frac{1}{((1+\lambda)m+1)^{\frac{1}{3}}(1+\lambda)^{\frac{2}{3}}m^{\frac{2}{3}}}\left(\frac{\eta}{2-\eta}\right)^{\frac{2}{3}},$$

$$m\,\xi(m, \lambda m, \eta) = \frac{m^{\frac{1}{3}}}{((1+\lambda)m+1)^{\frac{1}{3}}(1+\lambda)^{\frac{2}{3}}}\left(\frac{\eta}{2-\eta}\right)^{\frac{2}{3}} < \frac{1}{1+\lambda}. \tag{22}$$

Putting the first line into (8), the inequality (8) can be rewritten

$$\frac{2\eta^{\frac{2}{3}}}{3}\left[(J(\lambda m\,\xi(m, \lambda m, \eta)) - 1) + \lambda\,(J(m\,\xi(m, \lambda m, \eta)) - 1)\right]$$
$$< (2-\eta)^{\frac{2}{3}}\lambda m\left(1 - \left(1 + \frac{1}{(1+\lambda)m}\right)^{\frac{1}{3}}\right) + \min\left\{\lambda m(2^{\frac{2}{3}} - (2-\eta)^{\frac{2}{3}}), 2^{\frac{2}{3}} - \eta^{\frac{2}{3}}\right\}. \tag{23}$$

Using (22) and the fact that $J(0) = 1$, J is monotonically increasing on $[0, 1)$ (see [5, Appendix]), the first line in (23) is bounded from above by

$$\frac{2}{3}\left[\left(J\left(\frac{\lambda}{1+\lambda}\right) - 1\right) + \lambda\left(J\left(\frac{1}{1+\lambda}\right) - 1\right)\right]$$
$$< \frac{2}{3}\left[\left(J\left(\frac{3}{4}\right) - 1\right) + 3\left(J\left(\frac{1}{2}\right) - 1\right)\right] \ (\approx 0.2907).$$

According to the definition of $\overline{m}$ we have

$$\min\left\{\lambda m(2^{\frac{2}{3}} - (2-\eta)^{\frac{2}{3}}), 2^{\frac{2}{3}} - \eta^{\frac{2}{3}}\right\} = 2^{\frac{2}{3}} - \eta^{\frac{2}{3}},$$

from which the second line in (23) is bounded from below by

$$2^{\frac{2}{3}} - \eta^{\frac{2}{3}} - (2-\eta)^{\frac{2}{3}}\lambda m\left(\left(1 + \frac{1}{(1+\lambda)m}\right)^{\frac{1}{3}} - 1\right) > 2^{\frac{2}{3}} - \eta^{\frac{2}{3}} - (2-\eta)^{\frac{2}{3}}\frac{\lambda}{3(1+\lambda)}$$
$$\geq 2^{\frac{2}{3}} - \eta^{\frac{2}{3}} - \frac{1}{4}(2-\eta)^{\frac{2}{3}}.$$

Therefore, the inequality (23) follows easily if the function

$$2^{\frac{2}{3}} - \eta^{\frac{2}{3}} - \frac{1}{4}(2-\eta)^{\frac{2}{3}} - \frac{2}{3}\left[\left(J\left(\frac{3}{4}\right) - 1\right) + 3\left(J\left(\frac{1}{2}\right) - 1\right)\right]$$

is positive for every $\eta \in (0, 1]$. The minimum of this function on $(0, 1]$ occurs at $\eta = 1$ and the minimum value (≈ 0.0467) is indeed positive. This concludes the proof of Proposition 5. □

We remark here that Proposition 5 manifests what we asserted earlier: Theorem 1 is a substantial extension of the main result in [5]. It can be easily verified that, in [5, Theorem 5] the region of admissible masses is bounded for most $\phi \in (0, \pi]$ and the region diminishes when ϕ is smaller than 0.38π, see Fig. 3 for examples. In [5] the angle ϕ is confined to $\phi \leq \pi$ but it can actually be extended to $\phi \approx 1.16\pi$. In contrast, for any $\phi \in (0, \pi]$, our theorem holds for "most" choices of masses. As ϕ increases beyond π, the region of admissible masses remains nonempty until $\phi \approx 1.38\pi$.

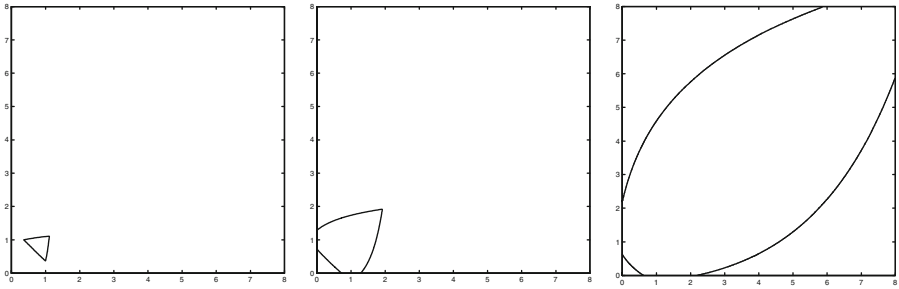

Fig. 3. Regions of admissible masses given by [5, Theorem 5] with ϕ equal (from left to right) 0.5π, 0.8π, 0.97π. Masses in these figures are bounded by $0 < m_1, m_2 \leq 8$

5. Retrograde Orbits with Various ϕ

The purpose of this section is to show miscellaneous samples of action-minimizing retrograde solutions obtained in Theorem 1. This family of solutions are determined by three parameters: m_1, m_2, ϕ. Tables of figures here are listed in the order of increasing ϕ, masses $m_1 \leq m_2$ are selected to illustrate deformation of action-minimizing orbits as mass parameters vary.

Masses (m_1, m_2) are mostly selected from the following lists, in which (m_1, m_2) are aligned in the same order as the figures.

(A)	(0.2, 0.8)	(0.4, 0.8)	(0.6, 0.8)	(0.8, 0.8)	(B)	(1, 7)	(3, 7)	(5, 7)	(7, 7)
	(0.2, 0.6)	(0.4, 0.6)	(0.6, 0.6)			(1, 5)	(3, 5)	(5, 5)	
	(0.2, 0.4)	(0.4, 0.4)				(1, 3)	(3, 3)		
	(0.2, 0.2)					(1, 1)			
(C)	(0.01, 4)	(0.1, 4)	(0.5, 4)	(0.8, 4)	(D)	(1, 100)	(10, 100)	(50, 100)	(100, 100)
	(0.01, 1)	(0.1, 1)	(0.5, 1)	(0.8, 1)					

Lists (A) and (B) contain typical examples of masses with $m_1 \leq m_2 < 1$ and $1 \leq m_1 \leq m_2$. Numerical figures corresponding to lists (C), (D) illustrate how action-minimizing orbits deform when $m_1 \ll 1 \leq m_2$ or $1 \ll m_2$. A more complete catalog of action-minimizing retrograde orbits is available at [13].

There is a total of 129 examples in this section, not all of them are covered by Theorem 1, but nonetheless we put them in for the entirety of our graphics. Seventeen examples in here fail to fulfill requirements in Theorem 1, ten of them are covered by Theorem 2, another three of them can be obtained by choosing other test paths. The remaining four examples without existence proof are:

$$(m_1, m_2, \phi) = (0.2, 0.6, 2\pi/3),\ (0.2, 0.4, 2\pi/3),\ (0.2, 0.4, 3\pi/4),\ (0.2, 0.4, 4\pi/5).$$

All of these examples belong to class (B).

For brevity we put numerical data for all of our examples, such as their initial conditions and action values, in the Appendix.

In Fig. 18 we skip the case $(m_1, m_2, \phi) = (1, 100, \pi)$ not only because this case is not covered by our theorems, but also because we don't think such a retrograde orbit can even exist. If one looks at the trajectory of the first body on the rotating frame, the loop deform across the third body as m_1 decreases from 10 to 1, resulting in a solution in a different topological class.

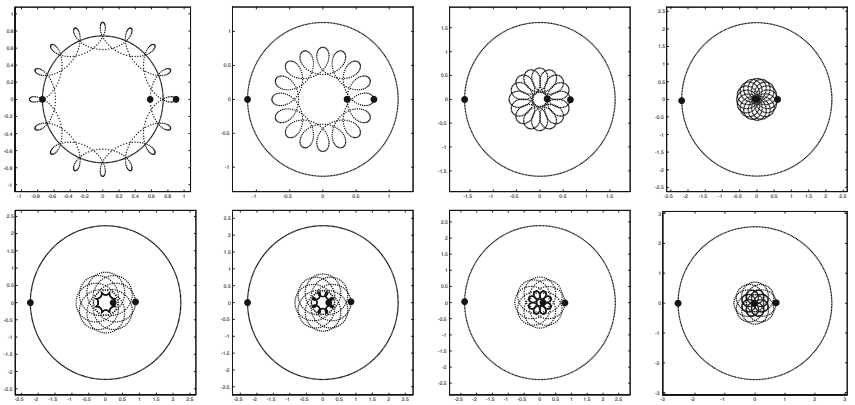

Fig. 4. Action minimizing retrograde solutions with masses $(m_1, m_2) = (0.5, 0.5), (1, 1), (2, 2), (4, 4)$ (first row), $(0.5, 8), (1, 8), (2, 8), (4, 8)$ (second row), $\phi = \pi/4$

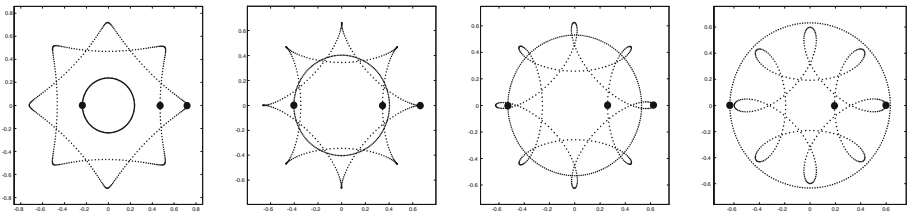

Fig. 5. Action minimizing retrograde solutions with masses $(m_1, m_2) = (0.2, 0.2), (0.4, 0.4), (0.6, 0.6), (0.8, 0.8)$, $\phi = \pi/2$

6. Proof of Theorem 2

The proof for Theorem 2 is similar to that of Theorem 1 but with some subtle improvements on the lower bound estimates for $\mathcal{A}$ over collision paths.

As observed in Sect. 2, the action functional $\mathcal{A}$ attains its infimum on the weak closure of $R_\phi \cap H_\phi^{\langle\sigma,\tau\rangle}$. All we need to show is that, under the assumptions of ϕ and masses in Theorem 2,

$$\inf_{x \in R_\phi \cap H_\phi^{\langle\sigma,\tau\rangle}} \mathcal{A}(x) < \inf_{x \in \partial R_\phi \cap H_\phi^{\langle\sigma,\tau\rangle}} \mathcal{A}(x), \tag{24}$$

and hence action minimizers do not fall on the weak boundary $\partial R_\phi \cap H_\phi^{\langle\sigma,\tau\rangle}$ of $R_\phi \cap H_\phi^{\langle\sigma,\tau\rangle}$.

Given $x \in R_\phi \cap H_\phi^{\langle\sigma,\tau\rangle}$, according to τ-invariance and the definition of H_ϕ,

$$x(t) = \overline{x(-t)} = \overline{e^{-\frac{\phi}{2}i}(x_2, x_1, x_3)(-t + \frac{1}{2})},$$

where hence

$$e^{-\frac{\phi}{4}i}x(t) = \overline{e^{-\frac{\phi}{4}i}(x_2, x_1, x_3)(-t + \frac{1}{2})}. \tag{25}$$

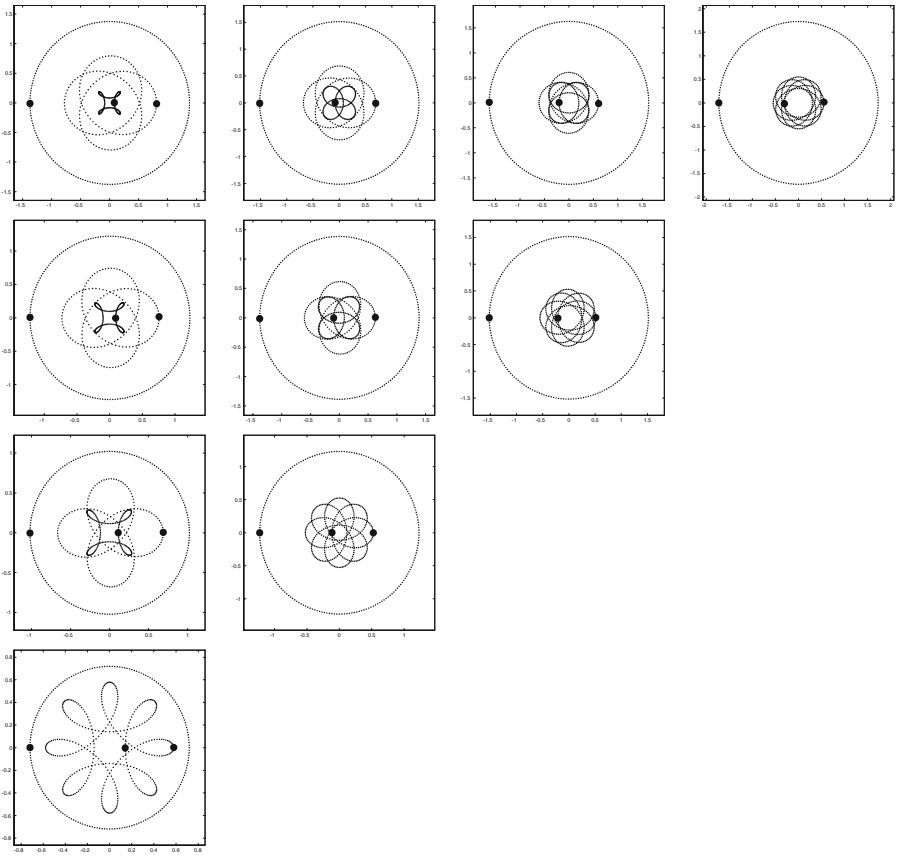

Fig. 6. Action minimizing retrograde solutions with (m_1, m_2) in (B), $\phi = \pi/2$

Combining with (17), we see that $[0, \frac{1}{4}]$ is a fundamental domain of the $\langle\sigma, \tau\rangle$-action; $x_1(t)$ and $x_2(-t+\frac{1}{2})$ are symmetric with respect to the line $L_{\frac{\phi}{4}} = \{re^{\frac{\phi}{4}i} : r \in \mathbb{R}\}$ as well as $x_2(t)$ and $x_1(-t+\frac{1}{2})$, and the same for the curves $x_3(t)$ and $x_3(-t+\frac{1}{2})$. In particular, $x_1(\frac{1}{4})$ and $x_2(\frac{1}{4})$ are symmetric with respect to $L_{\frac{\phi}{4}}$. Moreover, for any $t \in [0, \frac{1}{4}]$,

$$|x_1(t) - x_2(t)| = |x_1(-t+\frac{1}{2}) - x_2(-t+\frac{1}{2})|,$$
$$|\dot{x}_1(t) - \dot{x}_2(t)| = |\dot{x}_1(-t+\frac{1}{2}) - \dot{x}_2(-t+\frac{1}{2})|,$$

implying that

$$I_{1,M,\frac{1}{2}}(x_1 - x_2) = 2I_{1,M,\frac{1}{4}}(x_1 - x_2), \tag{26}$$

where $M = 2m + 1$ is the total mass.

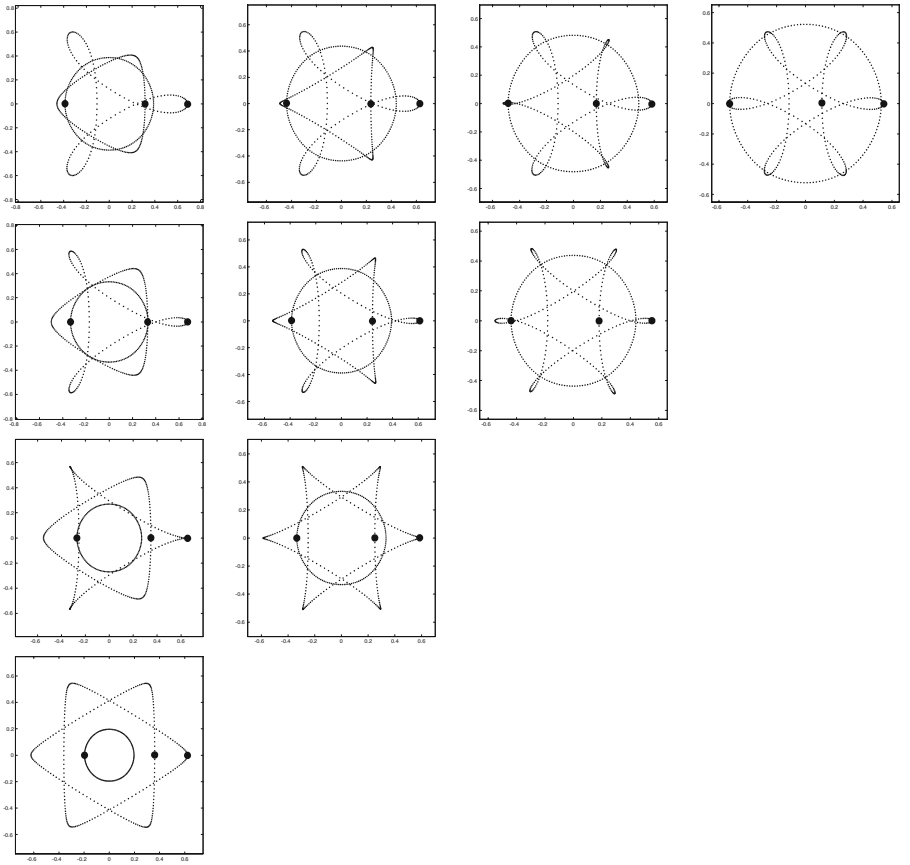

Fig. 7. Action minimizing retrograde solutions with (m_1, m_2) in (A), $\phi = 2\pi/3$

Suppose $x \in \partial R_\phi$, then $x_i(t) = x_j(t)$ for some $t \in [0, \frac{1}{4}]$ and $i \neq j$. One possibility is $i = 1$, $j = 2$. In this case,

$$x_1 - x_2 \in \Gamma^*_{\frac{1}{4}, \frac{\pi}{2} - \frac{\phi}{4}} \text{ or } \Gamma^*_{\frac{1}{4}, \frac{\pi}{2} + \frac{\phi}{4}},$$
$$x_1 - x_3,\ x_2 - x_3 \in \Gamma_{\frac{1}{2}, \frac{\phi}{2}} \text{ or } \Gamma_{\frac{1}{2}, \pi - \frac{\phi}{2}}.$$

As discussed in Sect. 3, due to our topological assumption, the case $x_1 - x_3 \in \Gamma_{\frac{1}{2}, \pi - \frac{\phi}{2}}$ (or $x_2 - x_3 \in \Gamma_{\frac{1}{2}, \pi - \frac{\phi}{2}}$) forces $x_1 - x_3$ (or $x_2 - x_3$) to fall into the space $\Gamma^*_{\frac{1}{2}, \pi - \frac{\phi}{2}}$. Therefore, for any $\phi \in (0, 2\pi)$, $I_{1, M, \frac{1}{2}}(x_1 - x_3)$ and $I_{1, M, \frac{1}{2}}(x_2 - x_3)$ are both bounded from below by

$$\frac{3}{4} M^{\frac{2}{3}} \phi^{\frac{2}{3}}.$$

By (2), Proposition 4, (17), (25), and (26),

$$\mathcal{A}(x) = \frac{2}{M} \sum_{i<j} m_i m_j \int_0^{\frac{1}{2}} \frac{1}{2} |\dot{x}_i - \dot{x}_j|^2 + \frac{M}{|x_i - x_j|}\, dt$$

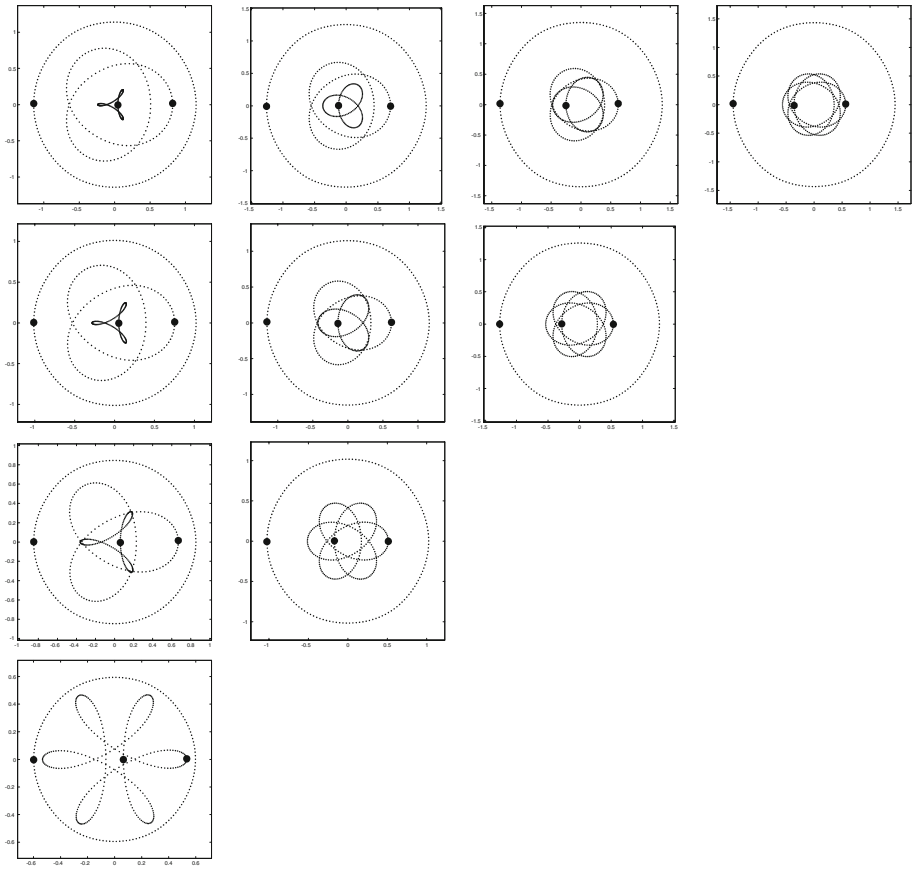

Fig. 8. Action minimizing retrograde solutions with (m_1, m_2) in (B), $\phi = 2\pi/3$

$$
\begin{aligned}
&= \frac{2}{M}\left[2m^2\, I_{1,M,\frac{1}{4}}(x_1 - x_2) + m\, I_{1,M,\frac{1}{2}}(x_1 - x_3) + m\, I_{1,M,\frac{1}{2}}(x_2 - x_3)\right] \\
&\geq \frac{2m}{M}\left[3mM^{\frac{2}{3}}\pi^{\frac{2}{3}}\left(\frac{1}{4}\right)^{\frac{1}{3}} + \frac{3}{2}M^{\frac{2}{3}}\phi^{\frac{2}{3}}\right] \\
&= 3m\left(\frac{\pi^2}{M}\right)^{\frac{1}{3}}\left[2^{\frac{1}{3}}m + \eta^{\frac{2}{3}}\right].
\end{aligned}
$$

The second possibility is $i = 1$, $j = 3$. In this case, by the τ-invariance x_2 and x_3 also collide at some $t \in [\frac{1}{4}, \frac{1}{2}]$. Therefore,

$$
\begin{aligned}
x_1 - x_2 &\in \Gamma_{\frac{1}{4},\frac{\pi}{2}-\frac{\phi}{4}} \text{ or } \Gamma_{\frac{1}{4},\frac{\pi}{2}+\frac{\phi}{4}}, \\
x_1 - x_3,\ x_2 - x_3 &\in \Gamma^*_{\frac{1}{2},\frac{\phi}{2}} \text{ or } \Gamma^*_{\frac{1}{2},\pi-\frac{\phi}{2}}.
\end{aligned}
$$

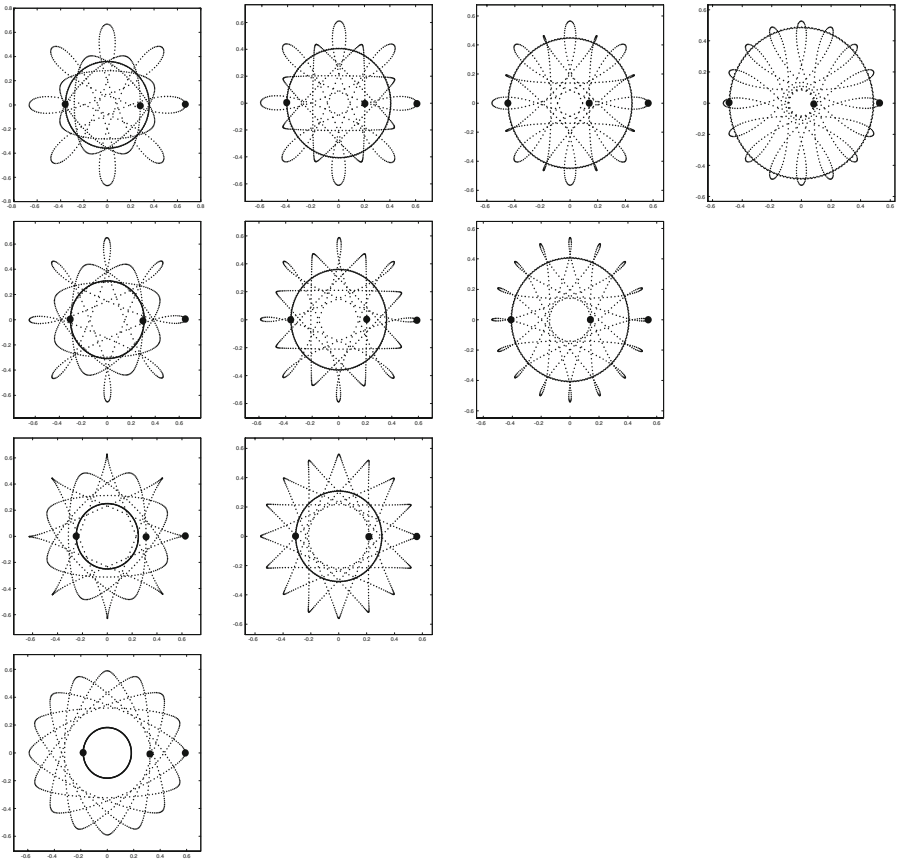

Fig. 9. Action minimizing retrograde solutions with (m_1, m_2) in (A), $\phi = 3\pi/4$

Then

$$\begin{aligned}
\mathcal{A}(x) &= \frac{2}{M}\sum_{i<j} m_i m_j \int_0^{\frac{1}{2}} \frac{1}{2}|\dot{x}_i - \dot{x}_j|^2 + \frac{M}{|x_i - x_j|}\,dt \\
&= \frac{2}{M}\left[2m^2\, I_{1,M,\frac{1}{4}}(x_1 - x_2) + m\, I_{1,M,\frac{1}{2}}(x_1 - x_3) + m\, I_{1,M,\frac{1}{2}}(x_2 - x_3)\right] \\
&\geq \frac{2m}{M}\left[3mM^{\frac{2}{3}}\left(\frac{\pi}{2} - \frac{\phi}{4}\right)^{\frac{2}{3}}\left(\frac{1}{4}\right)^{\frac{1}{3}} + \frac{3}{2}M^{\frac{2}{3}}\pi^{\frac{2}{3}}\left(\frac{1}{2}\right)^{\frac{1}{3}} + \frac{3}{2}M^{\frac{2}{3}}\pi^{\frac{2}{3}}\left(\frac{1}{2}\right)^{\frac{1}{3}}\right] \\
&= 3m\left(\frac{\pi^2}{M}\right)^{\frac{1}{3}}\left[\frac{m}{2}(2-\eta)^{\frac{2}{3}} + 2^{\frac{2}{3}}\right].
\end{aligned}$$

The estimate for the third possibility $i = 2$, $j = 3$ is identical.

Summarizing these estimates, we conclude that

$$\inf_{x\in\partial R_\phi \cap H_\phi^{\langle\sigma,\tau\rangle}} \mathcal{A}(x) \geq 3m\left(\frac{\pi^2}{M}\right)^{\frac{1}{3}} \min\left\{2^{\frac{1}{3}}m + \eta^{\frac{2}{3}},\ \frac{m}{2}(2-\eta)^{\frac{2}{3}} + 2^{\frac{2}{3}}\right\}. \qquad (27)$$

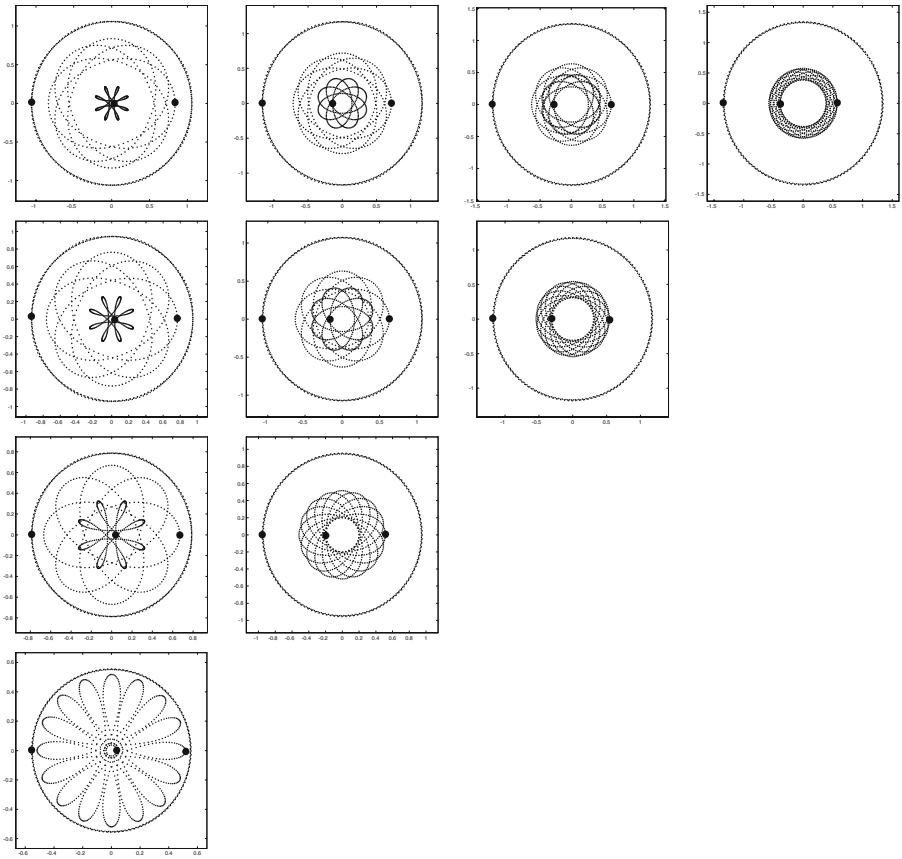

Fig. 10. Action minimizing retrograde solutions with (m_1, m_2) in (B), $\phi = 3\pi/4$

This provides a lower bound estimate for the right side of (24).

Observe that the path $x^{(\phi)}$ given in (20) belongs to $H_\phi^{\langle\sigma,\tau\rangle}$. It actually belongs to R_ϕ because (10) is identical to (7) in our case. Therefore, writing $\xi = \xi(m, m, \eta)$ and by (21),

$$\begin{aligned}
&\inf_{x\in R_\phi\cap H_\phi^{\langle\sigma,\tau\rangle}} \mathcal{A}(x)\\
&\le \left(\frac{\eta^2\pi^2}{M}\right)^{\frac{1}{3}}\left[\frac{3m_1m_2}{2(m_1+m_2)\xi}+\frac{3(m_1+m_2)}{2}+m_1\left(J\left(m_2\xi\right)-1\right)+m_2\left(J\left(m_1\xi\right)-1\right)\right]\\
&= m\left(\frac{\eta^2\pi^2}{M}\right)^{\frac{1}{3}}\left[\frac{3}{4\xi}+1+2J\left(m\xi\right)\right]. \qquad (28)
\end{aligned}$$

The assumption (11) is equivalent to that of the upper bound estimate in (28) and is strictly less than the lower bound estimate in (27). Therefore (11) implies (24). This completes the proof for Theorem 2.

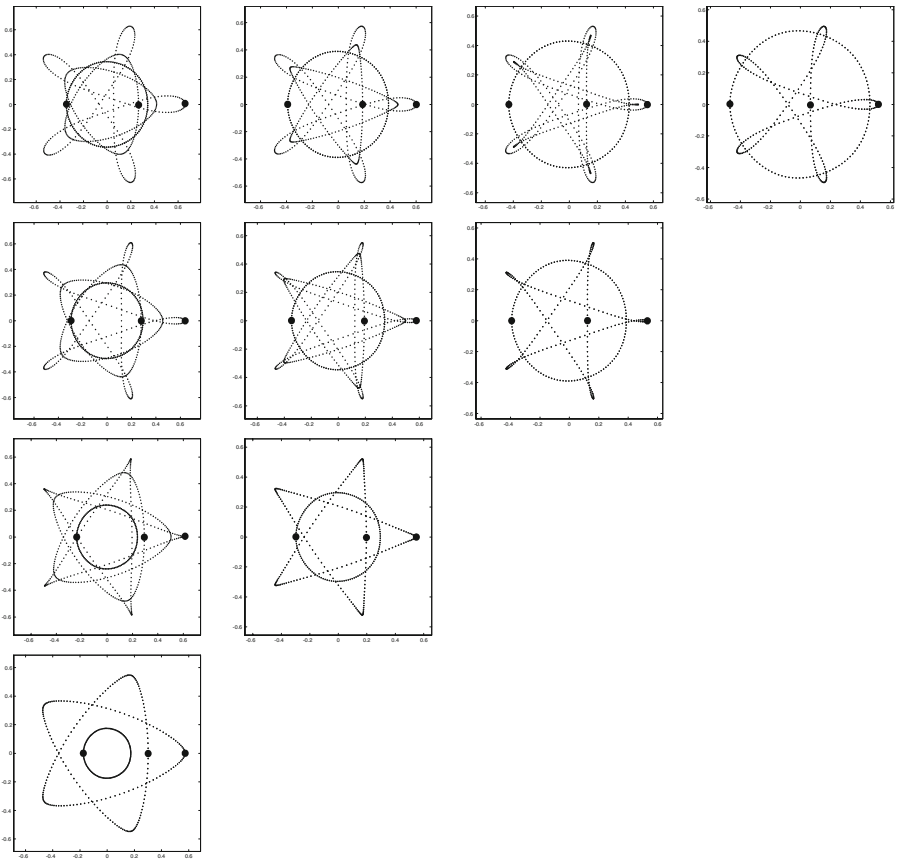

Fig. 11. Action minimizing retrograde solutions with (m_1, m_2) in (A), $\phi = 4\pi/5$

7. Proof of Theorem 3

The proof for Theorem 3 is similar to that of Theorem 2 but a prograde test path with action value larger than that of $x^{(\phi)}$ is inevitable. On the other hand, due to the topological nature of prograde paths, the lower bound estimate on collision paths can also be slightly improved.

As discussed before, the action functional $\mathcal{A}$ attains its infimum on the weak closure of $P_\phi \cap H_\phi^{\langle\sigma,\tau\rangle}$ and what we need to show is that

$$\inf_{x\in P_\phi\cap H_\phi^{\langle\sigma,\tau\rangle}} \mathcal{A}(x) < \inf_{x\in \partial P_\phi\cap H_\phi^{\langle\sigma,\tau\rangle}} \mathcal{A}(x) \tag{29}$$

under the assumptions of ϕ and masses in Theorem 3.

Let us first see how a "good" lower bound estimate for the right side of (29) can be obtained. The estimate (27) is valid for $\mathcal{A}$ on $\partial P_\phi \cap H_\phi^{\langle\sigma,\tau\rangle}$ as well, but we can do a bit better than that. If $x \in P_\phi \cap H_\phi^{\langle\sigma,\tau\rangle}$, then clearly (17), (25), and (26) hold since they are valid for any path in $H_\phi^{\langle\sigma,\tau\rangle}$.

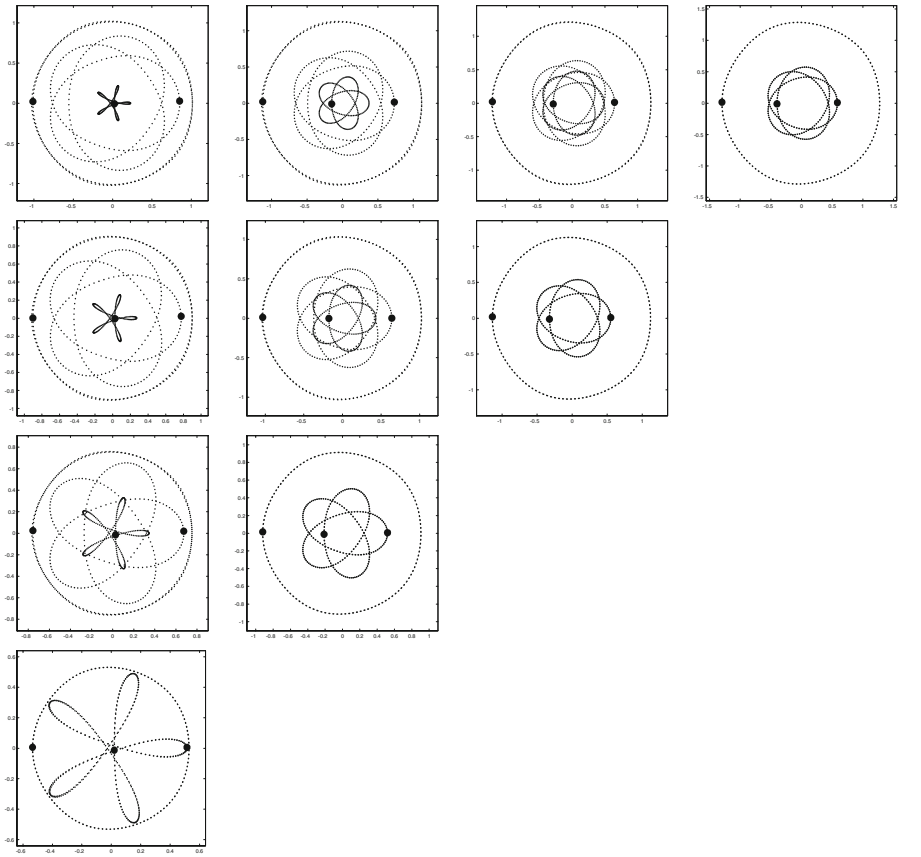

Fig. 12. Action minimizing retrograde solutions with (m_1, m_2) in (B), $\phi = 4\pi/5$

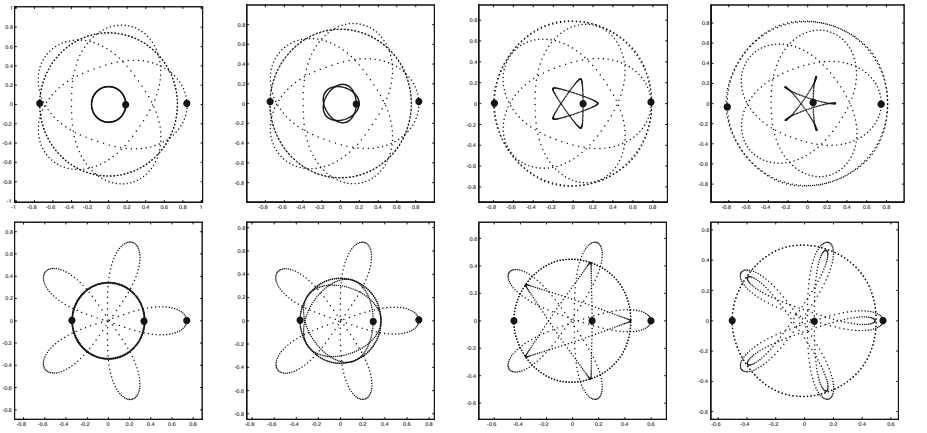

Fig. 13. Action minimizing retrograde solutions with (m_1, m_2) in (C), $\phi = 4\pi/5$

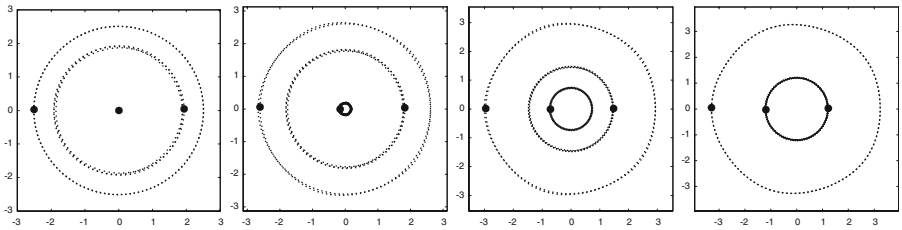

Fig. 14. Action minimizing retrograde solutions with (m_1, m_2) in (D), $\phi = 4\pi/5$

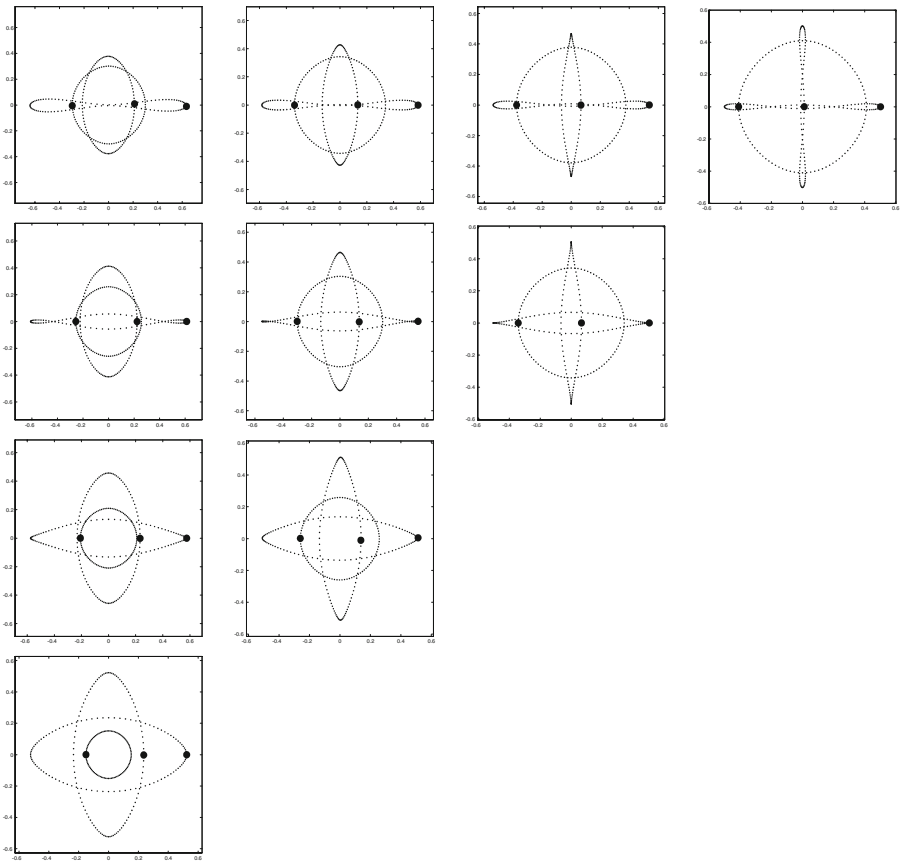

Fig. 15. Action minimizing retrograde solutions with (m_1, m_2) in (A), $\phi = \pi$

Suppose $x \in \partial P_\phi$, then $x_i(t) = x_j(t)$ for some $t \in [0, \frac{1}{4}]$ and $i \neq j$. The estimate for the first possibility $i = 1$, $j = 2$ is the same as the one obtained in Sect. 6:

$$\mathcal{A}(x) \geq 3m \left(\frac{\pi^2}{M}\right)^{\frac{1}{3}} \left[2^{\frac{1}{3}} m + \eta^{\frac{2}{3}}\right].$$

As before, $M = 2m + 1$ denotes the total mass.

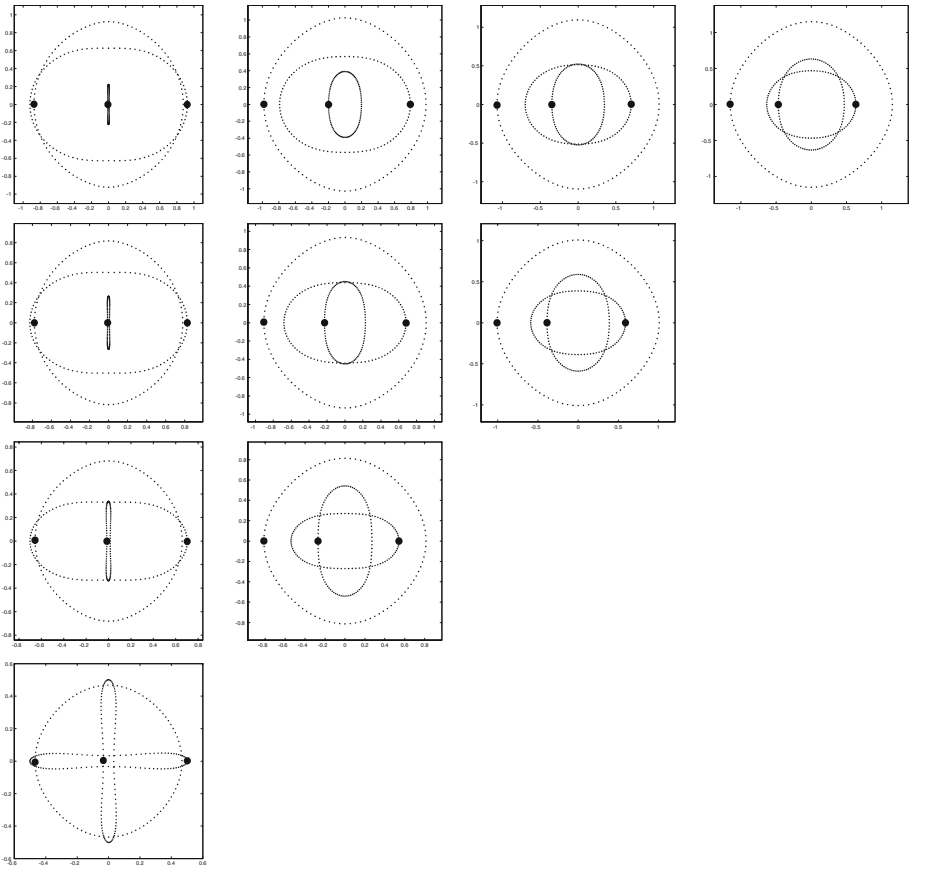

Fig. 16. Action minimizing retrograde solutions with (m_1, m_2) in (B), $\phi = \pi$

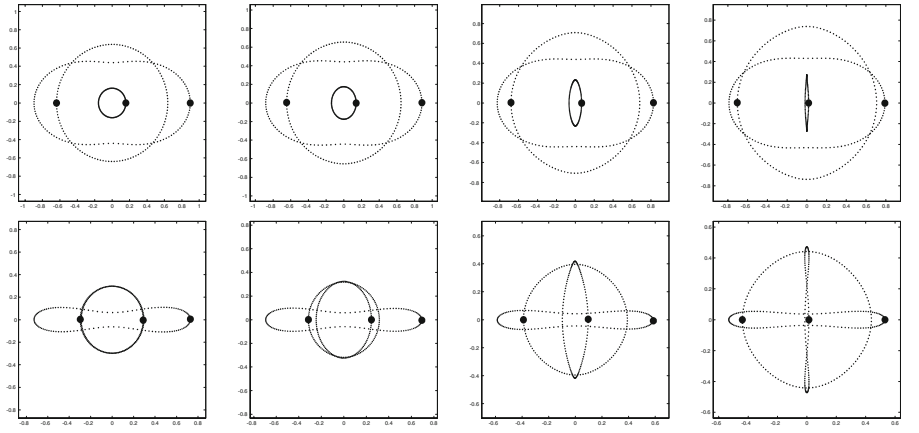

Fig. 17. Action minimizing retrograde solutions with (m_1, m_2) in (C), $\phi = \pi$

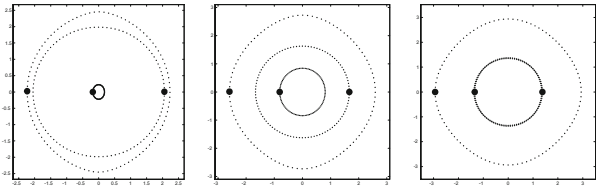

Fig. 18. Action minimizing retrograde solutions with (m_1, m_2) in (D), $\phi = \pi$, except the case $(m_1, m_2) = (1, 100)$

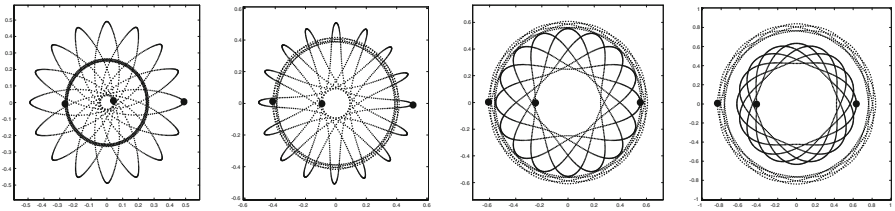

Fig. 19. Action minimizing retrograde solutions with $\phi = 5\pi/4$ and $(m_1, m_2) = (0.5, 0.5), (1, 1), (2, 2), (4, 4)$

The second possibility we consider is that $x_1(t) = x_3(t)$ for some $t \in [0, \frac{1}{4}]$ and $x_1(t) \neq x_2(t)$ for any $t \in [0, \frac{1}{4}]$. We claim that in this case we must have

$$x_1 - x_2 \in \Gamma_{\frac{1}{4}, \frac{\pi}{2}+\frac{\phi}{4}}.$$

To see this, consider any sequence $x^{(n)}$ in $P_\phi \cap H_\phi^{\langle\sigma,\tau\rangle}$ which converges weakly to $x \in \partial P_\phi$. The symmetry conditions (17) and (25) force $x_1^{(n)} - x_2^{(n)}$, for each n, to turn an angle $\frac{\pi}{2}$ counterclockwise on the rotating frame, and thus turn an angle $\frac{\pi}{2} + \frac{\phi}{4}$ counterclockwise on the inertia frame. But since $x_1^{(n)} - x_2^{(n)}$ converges uniformly on $[0, \frac{1}{4}]$ to $x_1 - x_2$ which stays away from the origin for $t \in [0, \frac{1}{4}]$, $x_1 - x_2$ also turns an angle $\frac{\pi}{2}$ counterclockwise on the rotating frame and an angle $\frac{\pi}{2} + \frac{\phi}{4}$ counterclockwise on the inertia frame. This proves what we just claimed. Since x is τ-invariant, x_2 and x_3 collide at some $t \in [\frac{1}{4}, \frac{1}{2}]$ and therefore

$$x_1 - x_3,\ x_2 - x_3 \in \Gamma^*_{\frac{1}{2}, \frac{\phi}{2}} \ \text{ or } \ \Gamma^*_{\frac{1}{2}, \pi - \frac{\phi}{2}}.$$

Then by (2), Proposition 4, (17), (25), and (26),

$$\begin{aligned}
\mathcal{A}(x) &= \frac{2}{M} \sum_{i<j} m_i m_j \int_0^{\frac{1}{2}} \frac{1}{2} |\dot{x}_i - \dot{x}_j|^2 + \frac{M}{|x_i - x_j|}\, dt \\
&= \frac{2}{M} \left[2m^2\, I_{1,M,\frac{1}{4}}(x_1 - x_2) + m\, I_{1,M,\frac{1}{2}}(x_1 - x_3) + m\, I_{1,M,\frac{1}{2}}(x_2 - x_3) \right] \\
&\geq \frac{2m}{M} \left[3m M^{\frac{2}{3}} \left(\frac{\pi}{2} + \frac{\phi}{4} \right)^{\frac{2}{3}} \left(\frac{1}{4} \right)^{\frac{1}{3}} + \frac{3}{2} M^{\frac{2}{3}} \pi^{\frac{2}{3}} \left(\frac{1}{2} \right)^{\frac{1}{3}} + \frac{3}{2} M^{\frac{2}{3}} \pi^{\frac{2}{3}} \left(\frac{1}{2} \right)^{\frac{1}{3}} \right] \\
&= 3m \left(\frac{\pi^2}{M} \right)^{\frac{1}{3}} \left[\frac{m}{2} (2 + \eta)^{\frac{2}{3}} + 2^{\frac{2}{3}} \right].
\end{aligned}$$

The remaining possibility is that $x_2(t) = x_3(t)$ for some $t \in [0, \frac{1}{4}]$ and $x_1(t) \neq x_2(t)$ for any $t \in [0, \frac{1}{4}]$. The resulting lower bound estimate for $\mathcal{A}(x)$ is clearly the same as the second possibility.

Summarizing these estimates, we conclude that

$$\inf_{x \in \partial P_\phi \cap H_\phi^{\langle \sigma, \tau \rangle}} \mathcal{A}(x) \geq 3m \left(\frac{\pi^2}{M}\right)^{\frac{1}{3}} \min \left\{ 2^{\frac{1}{3}} m + \eta^{\frac{2}{3}},\ \frac{m}{2}(2+\eta)^{\frac{2}{3}} + 2^{\frac{2}{3}} \right\}. \tag{30}$$

This provides a lower bound estimate for the right side of (29). It is sharper than (27) for the boundary of retrograde paths.

Now we take a prograde test path modified from $x^{(\phi)}$ in (20) to acquire a good upper bound estimate for the left side of (29). Let

$$\begin{aligned} Q(t) &:= \frac{1}{(M\phi)^{\frac{2}{3}}} e^{\phi t i}, \\ P(t) &:= \frac{1}{(2m)^{\frac{2}{3}}(2\pi+\phi)^{\frac{2}{3}}} e^{(\phi+2\pi)ti}, \end{aligned}$$

and consider an artificial path

$$\begin{aligned} y^{(\phi)}(t) &= (y_1^{(\phi)}(t), y_2^{(\phi)}(t), y_3^{(\phi)}(t)) \\ &:= (Q(t) + mP(t),\ Q(t) - mP(t),\ -2m\, Q(t)). \end{aligned} \tag{31}$$

Then $y^{(\phi)}$ has the same initial ordering as $x^{(\phi)}$ and fulfills the requirement in the definition of $C_\phi^\dagger$. Particles $y_1^{(\phi)}$ and $y_2^{(\phi)}$ revolve counterclockwise about their mass center $Q(t)$ along circular paths, while $Q(t)$ and $y_3^{(\phi)}$ revolve counterclockwise along circular paths about the origin, the mass center of $y^{(\phi)}$. The path $y^{(\phi)}$ belongs to $H_\phi^{\langle \sigma, \tau \rangle}$, as does $x^{(\phi)}$. Note that $\eta \in (0, 2)$ implies

$$\left(\frac{\phi}{2(2\pi+\phi)}\right)^{\frac{2}{3}} = \left(\frac{\eta}{2(2+\eta)}\right)^{\frac{2}{3}} < \left(2 + \frac{1}{m}\right)^{\frac{1}{3}} = \left(\frac{M}{m}\right)^{\frac{1}{3}}.$$

Equivalently,

$$m|P(t)| = \frac{m}{(2m)^{\frac{2}{3}}(2\pi+\phi)^{\frac{2}{3}}} < \left(\frac{M}{\phi^2}\right)^{\frac{1}{3}} = M|Q(t)|,$$

which ensures that $y_3^{(\phi)}$ stays away from the binary $y_1^{(\phi)}, y_2^{(\phi)}$. This implies $y^{(\phi)} \in P_\phi$.

Similar to the calculations for $K(\dot{x}^{(\phi)})$, we have

$$\begin{aligned} K(\dot{y}^{(\phi)}) &= \frac{1}{2}\left[(m_1+m_2)\left(\frac{\phi^2}{M}\right)^{\frac{1}{3}} + \frac{m_1 m_2 (2\pi+\phi)^{\frac{2}{3}}}{(m_1+m_2)^{\frac{1}{3}}} \right] \\ &= \frac{1}{2}\left[2m\left(\frac{\phi^2}{M}\right)^{\frac{1}{3}} + \frac{m^2(2\pi+\phi)^{\frac{2}{3}}}{(2m)^{\frac{1}{3}}} \right]. \end{aligned}$$

The contribution of $U(y^{(\phi)})$ to the total action can be written

$$\begin{aligned}
&\int_0^1 U(y^{(\phi)})\,dt \\
&= \int_0^1 \frac{m^2}{|y_1^{(\phi)} - y_2^{(\phi)}|} + \frac{m}{|y_1^{(\phi)} - y_3^{(\phi)}|} + \frac{m}{|y_2^{(\phi)} - y_3^{(\phi)}|}\,dt \\
&= \int_0^1 \frac{m^2(2\pi+\phi)^{\frac{2}{3}}}{(2m)^{\frac{1}{3}}} + \left(\frac{\phi^2}{M}\right)^{\frac{1}{3}} \frac{m}{|1 - m\zeta e^{2\pi t i}|} + \left(\frac{\phi^2}{M}\right)^{\frac{1}{3}} \frac{m}{|1 - m\zeta e^{2\pi t i}|}\,dt \\
&= \frac{m^2(2\pi+\phi)^{\frac{2}{3}}}{(2m)^{\frac{1}{3}}} + 2m\left(\frac{\phi^2}{M}\right)^{\frac{1}{3}} J(m\zeta).
\end{aligned}$$

Here $\zeta = \zeta(m, \eta)$ is given in (12). Therefore,

$$\begin{aligned}
\inf_{x \in P_\phi \cap H_\phi^{\langle \sigma, \tau \rangle}} \mathcal{A}(x) &\le \frac{3m^2(2\pi+\phi)^{\frac{2}{3}}}{2(2m)^{\frac{1}{3}}} + \left(\frac{\phi^2}{M}\right)^{\frac{1}{3}} [m + 2mJ(m\zeta)] \qquad (32) \\
&= m\left(\frac{\eta^2\pi^2}{M}\right)^{\frac{1}{3}} \left[\frac{3}{4\zeta} + 1 + 2J(m\zeta)\right].
\end{aligned}$$

The assumption (13) is easily seen to be equivalent to that the upper bound estimate in (32) is strictly less than the lower bound estimate in (30). Therefore (13) implies (29). This completes the proof for Theorem 3.

8. Retrograde and Prograde Orbits with Additional Symmetries

The set of admissible (m, η) for action-minimizing retrograde orbits obtained by Theorem 2, where $m_1 = m_2 = m$ and $m_3 = 1$, is the region below the cliff-like curve in the first graph of Fig. 20. The nearly horizontal portion ($\eta \approx 1.45$) which cuts out admissible (m, η) with large η is due to the inequality (10). Similarly, the other graph of Fig. 20 shows the set of admissible (m, η) for action-minimizing prograde orbits obtained by Theorem 3. The region is given by a single inequality (13). Note that these two curves match at $\eta = 0$ since (11) and (13) are the same at this limiting case.

The variational problem studied throughout the paper can be also formulated as the minimization problem of the action functional over relative periodic loops in $C_{\phi,T}$ or $C^\dagger_{\phi,T}$ with $\phi \in (-2\pi, 2\pi)$. Retrograde paths in $C^\dagger_{\phi,T}$ are continuously deformed to prograde paths as ϕ (or η) decreases continuously from positive values to negative values. The borderline case $\phi = 0$ is the only case without action minimizer, since it is the only case without coercivity.

Figure 21 shows several numerical figures of action-minimizing prograde orbits obtained in Theorem 3. More action-minimizing prograde orbits with $m_1 = m_2$ can be found in [13]. Many examples of retrograde orbits with $m_1 = m_2$ are already included in Sect. 5. In the order of their appearance, the set of (m, η) in Fig. 21 are

		(1.5, 1.25)	(2, 1.25)
	(1, 1)	(1.5, 1)	(2, 1)
(0.5, 0.5)	(1, 0.5)	(1.5, 0.5)	(2, 0.5)
(0.5, 0.25)	(1, 0.25)	(1.5, 0.25)	(2, 0.25)

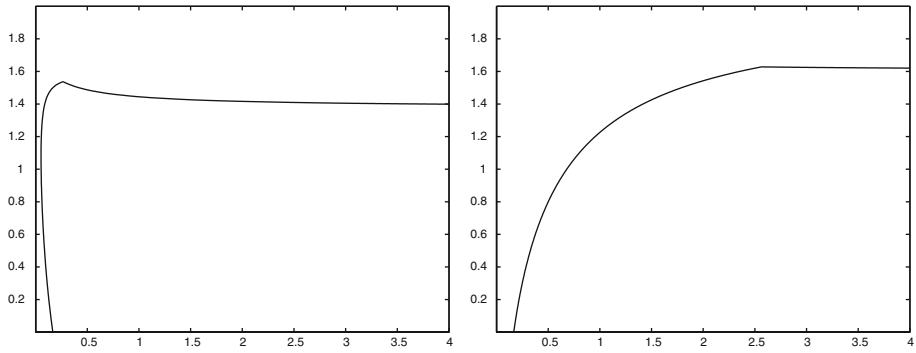

Fig. 20. Admissible (m, η) given by Theorem 2 and Theorem 3 for retrograde (left) and prograde (right) solutions in $H_\phi^{\langle\sigma,\tau\rangle}$

Numerical data for these orbits are listed on Table 18 in the Appendix. The cases (0.5, 1.25), (1, 1.25), (0.5, 1) are missing because they do not fall inside our region of admissible (m, η).

Similar to Proposition 5 we can now establish simple criteria for (m, η) to satisfy the requirements in Theorem 2 and Theorem 3. The criterion in Proposition 6 for retrograde orbits is far from sharp but it is easy to verify, and it shows in particular that the region of admissible (m, η) contains a large rectangle of the form $[m_0, \infty) \times (0, 1]$. Proposition 7 is similar to Proposition 6. For fixed m, as η approaches zero, our retrograde or prograde orbits link to classical results by analytic continuation near infinity (see [22] for references). For fixed η, as m approaches infinity, these orbits link to satellite orbits of some restricted n-body problems, which can also be obtained by the minimization method [6].

Proposition 6. *Let J be as in (4). For any $\phi = \eta\pi \in (0, 2\pi)$, inequalities (10),(11) hold whenever*

$$m \geq \frac{2^{\frac{2}{3}} - \eta^{\frac{2}{3}}}{2^{\frac{1}{3}} - \frac{1}{2}(2-\eta)^{\frac{2}{3}}} \quad \textit{and} \quad \eta \leq \frac{2\sqrt{2m+1}}{\sqrt{2m+1} + \sqrt{2m}}. \tag{33}$$

Proof. The first inequality in (33) is equivalent to

$$\min\left\{2^{\frac{1}{3}}m + \eta^{\frac{2}{3}},\ \frac{m}{2}(2-\eta)^{\frac{2}{3}} + 2^{\frac{2}{3}}\right\} = \frac{m}{2}(2-\eta)^{\frac{2}{3}} + 2^{\frac{2}{3}}.$$

Clearly (10) follows from the second inequality of (33), which also implies that

$$\eta^2 - 4(2m+1)\eta + 4(2m+1) \geq 0.$$

In fact the term on the right end of (33) is a root of this quadratic polynomial in η. Let ξ be as in (5) with $m_1 = m_2 = m$. Then the above inequality can be also written

$$m\xi = \frac{1}{2(1+\frac{1}{2m})^{\frac{1}{3}}}\left(\frac{\eta}{2-\eta}\right)^{\frac{2}{3}} \leq \frac{1}{2}.$$

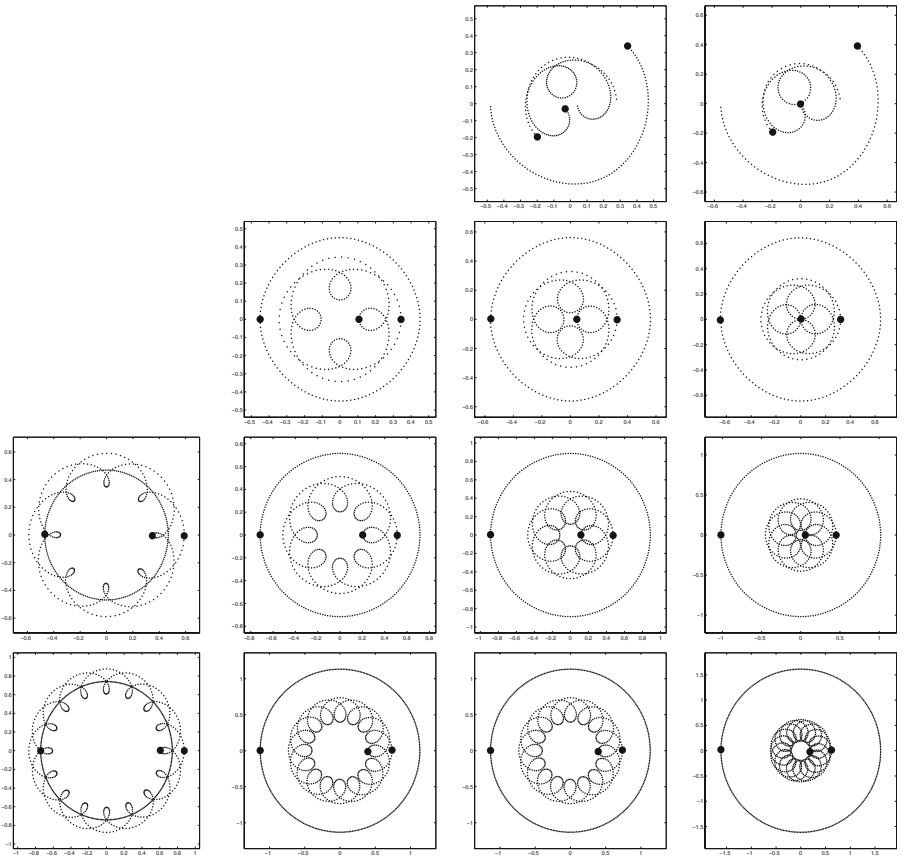

Fig. 21. Action-minimizing prograde orbits obtained in Theorem 3 with $m_1 \le m_2$

Recall that J is increasing on $[0, 1)$. Therefore

$$J(m\xi) \le J\left(\frac{1}{2}\right).$$

Note that the second inequality of (33) is always valid if $\eta \in (0, 1]$. When $\eta \in (1, 2)$, (33) can be written

$$\frac{2^{\frac{2}{3}} - \eta^{\frac{2}{3}}}{2^{\frac{1}{3}} - \frac{1}{2}(2-\eta)^{\frac{2}{3}}} \le m \le \frac{(2-\eta)^2}{2\left((2-\eta)^2 - \eta^2\right)}.$$

The inequality for the two expressions in η fails if, say $\eta \ge 3/2$. It can be easily verified that

$$2^{\frac{2}{3}} - \frac{\eta^{\frac{2}{3}}}{3}\left(1 + 2J\left(\frac{1}{2}\right)\right) - \frac{1}{12}(2-\eta)^{\frac{2}{3}} > 0$$

for $\eta \in (0, 3/2)$ (in fact, this inequality holds whenever $\eta < 1.8146$). From this observation we have

$$2^{\frac{2}{3}} - \frac{\eta^{\frac{2}{3}}}{3}\left(1 + 2J\left(\frac{1}{2}\right)\right) > \frac{1}{12}(2-\eta)^{\frac{2}{3}} > \frac{m}{2}\left(\left(1+\frac{1}{2m}\right)^{\frac{1}{3}} - 1\right)(2-\eta)^{\frac{2}{3}}.$$

Then

$$\begin{aligned} 2^{\frac{2}{3}} + \frac{m}{2}(2-\eta)^{\frac{2}{3}} &> \frac{\eta^{\frac{2}{3}}}{3}\left(1 + 2J\left(\frac{1}{2}\right)\right) + \frac{m}{2}\left(1+\frac{1}{2m}\right)^{\frac{1}{3}}(2-\eta)^{\frac{2}{3}} \\ &\geq \frac{\eta^{\frac{2}{3}}}{3}\left(1 + 2J\left(m\xi\right)\right) + \frac{\eta^{\frac{2}{3}}}{4\xi}. \end{aligned}$$

This proves (11). □

Proposition 7. *Let J be as in (4). For any $\phi = \eta\pi \in (0, 2\pi)$, inequality (13) holds whenever*

$$m \geq \frac{2^{\frac{2}{3}} - \eta^{\frac{2}{3}}}{2^{\frac{1}{3}} - \frac{1}{2}(2+\eta)^{\frac{2}{3}}} \quad \text{and} \quad 0 < 2^{\frac{2}{3}} - \frac{\eta^{\frac{2}{3}}}{3}\left(1 + 2J\left(\frac{1}{2}\right)\right) - \frac{1}{12}(2+\eta)^{\frac{2}{3}}. \tag{34}$$

Proof. The first inequality (34) is equivalent to

$$\min\left\{2^{\frac{1}{3}}m + \eta^{\frac{2}{3}},\ \frac{m}{2}(2+\eta)^{\frac{2}{3}} + 2^{\frac{2}{3}}\right\} = \frac{m}{2}(2+\eta)^{\frac{2}{3}} + 2^{\frac{2}{3}}.$$

Let ζ be as in (12) with $m_1 = m_2 = m$. Then $m\zeta$ is easily seen to be bounded from above by $1/2$ for every $\eta \in (0, 2)$. Following the last paragraph in the proof of Proposition 6, the inequality (34) is readily seen to imply (13). □

The special case $m = 1$ is connected to many numerical discoveries by Broucke [2] and Hénon [12]. In [12] Hénon shows the complete retrograde family for the special case $m_1 = m_2 = m_3 = 1$. As η decreases from 2 to a small positive number, the retrograde orbit deforms from Schubart's rectilinear orbit [20] to a retrograde orbit with a tight binary (see [12, Fig.1-3]). Part of this family and some prograde orbits with equal masses are also obtained by Broucke [2]. It is unknown whether this prograde family is continuable to $\eta = 2$ as the retrograde family. Classical methods on existence of such solutions apply to cases with small η.

Schubart's orbit has recently received some rigorous treatments via topological [16] and variational arguments [23]. This orbit falls on the boundary of retrograde paths in $C^{\dagger}_{2\pi}$ with x_2 bouncing back and forth between x_1 and x_3. Within the class of prograde and retrograde paths in $C^{\dagger}_{2\pi}$ there are numerical solutions [2, Fig.9-10] whose rigorous existence proofs are yet to be found.

9. Estimating Mutual Distances

This section is dedicated to providing quantitative estimates for the mutual distances of action-minimizing orbits. Action-minimizing retrograde solutions have no tight binaries, as we shall see in this section, and they are therefore different from those retrograde solutions obtained by classical perturbation arguments. A brief explanation for this fact

along with a crude estimate of upper and lower bounds for distance ratios can be found in [5, §6]. The estimates supplied here are finer.

Let $x \in R_\phi \cap H_\phi^{\langle\sigma\rangle}$ be an action-minimizing retrograde solution obtained in Theorem 1. Let

$$\bar{r}_{ij} = \max_{t\in[0,1]} |x_i(t) - x_j(t)|, \quad \underline{r}_{ij} = \min_{t\in[0,1]} |x_i(t) - x_j(t)|. \tag{35}$$

Writing $x_i - x_j$ in polar form $r_{ij}e^{i\theta_{ij}}$, then by σ-invariance and (17), $\theta_{ij}(\frac{1}{2}) - \theta_{ij}(0) = \frac{\phi}{2}$ or $\pi - \frac{\phi}{2}$. Let

$$\psi := \frac{\pi - |\pi - \phi|}{2} = \min\left\{\frac{\phi}{2}, \pi - \frac{\phi}{2}\right\}. \tag{36}$$

Then

$$\begin{aligned}
\int_0^{\frac{1}{2}} \frac{1}{2}|\dot{x}_i - \dot{x}_j|^2 + \frac{M}{|x_i - x_j|}\,dt &= \int_0^{\frac{1}{2}} \frac{1}{2}(\dot{r}_{ij}^2 + r_{ij}^2\dot{\theta}_{ij}^2) + \frac{M}{r_{ij}}\,dt \\
&\geq \left(\int_0^{\frac{1}{2}} |\dot{r}_{ij}|dt\right)^2 + \underline{r}_{ij}^2\left(\int_0^{\frac{1}{2}} |\dot{\theta}_{ij}|dt\right)^2 + \frac{M}{2\bar{r}_{ij}} \\
&\geq (\bar{r}_{ij} - \underline{r}_{ij})^2 + \underline{r}_{ij}^2\psi^2 + \frac{M}{2\bar{r}_{ij}} \\
&\geq \frac{\psi^2\bar{r}_{ij}^2}{\psi^2+1} + \frac{M}{2\bar{r}_{ij}}.
\end{aligned}$$

Consequently,

$$\begin{aligned}
\mathcal{A}(x) &= \frac{2}{M}\sum_{i<j} m_i m_j \int_0^{\frac{1}{2}} \frac{1}{2}|\dot{x}_i - \dot{x}_j|^2 + \frac{M}{|x_i - x_j|}\,dt \\
&\geq \frac{1}{M}\sum_{i<j} m_i m_j \left(\frac{2\psi^2\bar{r}_{ij}^2}{\psi^2+1} + \frac{M}{\bar{r}_{ij}}\right).
\end{aligned} \tag{37}$$

The elementary identity

$$\min_{s\in(0,\infty)}\left\{\left(\frac{2\psi^2}{\psi^2+1}\right)s^2 + \frac{M}{s}\right\} = \frac{3}{2}\left(\frac{4\psi^2M^2}{\psi^2+1}\right)^{\frac{1}{3}} \tag{38}$$

implies that, for any pair of $i < j$,

$$\mathcal{A}(x) \geq \frac{m_i m_j}{M}\left(\frac{2\psi^2\bar{r}_{ij}^2}{\psi^2+1} + \frac{M}{\bar{r}_{ij}}\right) + \frac{3}{2M}\left(\frac{4\psi^2M^2}{\psi^2+1}\right)^{\frac{1}{3}} \sum_{\substack{k<l \\ (k,l)\neq(i,j)}} m_k m_l. \tag{39}$$

For any fixed masses and ϕ (and hence ψ), the two positive solutions for the equation

$$\left(\frac{2\psi^2}{\psi^2+1}\right)s^2 + \frac{M}{s} = \left(\frac{M}{m_i m_j}\right)\mathcal{A}(x) - \frac{3}{2m_i m_j}\left(\frac{4\psi^2M^2}{\psi^2+1}\right)^{\frac{1}{3}} \sum_{\substack{k<l \\ (k,l)\neq(i,j)}} m_k m_l \tag{40}$$

in s are clearly lower and upper bounds for $\overline{r}_{ij}$. Summarizing these observations, we obtain:

Proposition 8. *Fix $m_1, m_2 > 0$, $\phi \in (0, 2\pi)$, and let x be an action-minimizing retrograde solution of the three-body problem in $R_\phi \cap H_\phi^{\langle\sigma\rangle}$ given by Theorem 1. Let $\overline{r}_{ij}$ and ψ be as in (35) and (36). Then for each pair of $i < j$ from $\{1, 2, 3\}$, the two positive solutions of identity (40) are lower and upper bounds for $\overline{r}_{ij}$.*

The practical way of applying Proposition 8 is to choose an ideal retrograde path x_{test} in $R_\phi \cap H_\phi^{\langle\sigma\rangle}$ and replace the $\mathcal{A}(x)$ in (40) by its upper bound $\mathcal{A}(x_{\text{test}}) = \mathcal{A}_{\text{test}}$. The resulting bounds for $\overline{r}_{ij}$ are of course not as sharp, but as indicated by the tables in the Appendix, the test paths selected in Sect. 3 whose action values were given in (21) provide fairly sharp upper bound estimates for $\mathcal{A}(x)$ for a wide range of masses and rotation angles. They often provide satisfactory approximations for the bounds given in Proposition 8. It is maybe surprising that the difference between the action value $\mathcal{A}(x)$ and $\mathcal{A}_{\text{test}}$ is within 0.3% (many of them differ by less than 0.1%!) among most of the examples given in this paper.

A recursive application of (37) leads to better estimates for mutual distances, as explained below. Let α_{ij} and β_{ij} denote the lower and upper bounds for $\overline{r}_{ij}$ obtained in Proposition 8. For example, the case $(m_1, m_2) = (3, 5)$ and $\phi = \pi$ gives

$$(\alpha_{12}, \beta_{12}) \approx (0.5320, 3.1920), \quad (\alpha_{23}, \beta_{23}) \approx (0.2690, 4.7163),$$
$$(\alpha_{13}, \beta_{13}) \approx (0.1809, 5.8235).$$

Among our examples the ratios β_{ij}/α_{ij} range mostly from 5 to 70. The estimates α_{ij} and β_{ij} for mutual distances can be refined by improving (39). The inequality (39) is obtained from (38), but with Proposition 8 we may write

$$\mathcal{A}(x) \geq \frac{m_i m_j}{M}\left(\frac{2\psi^2 \overline{r}_{ij}^2}{\psi^2+1} + \frac{M}{\overline{r}_{ij}}\right) + \sum_{\substack{k<l \\ (k,l)\neq(i,j)}} \frac{m_k m_l}{M}\left(\frac{2\psi^2 \alpha_{kl}^2}{\psi^2+1} + \frac{M}{\beta_{kl}}\right)$$

and rewrite (40) accordingly. Once the new lower and upper bound estimates for each $\overline{r}_{ij}$ were obtained, still denote them by α_{ij} and β_{ij}, then we may repeat this process and further improve the above inequality and α_{ij}, β_{ij}. Repetition of this process results in finer and finer estimates for mutual distances. Numerical calculations show that this procedure often lowers the ratios β_{ij}/α_{ij} by about 15%.

10. Appendix: Numerical Data

This Appendix contains numerical data for the orbits listed in Sect. 5 and 8. Most of the data in here are accurate to the fourth decimal place. Readers may reproduce most of the figures in Sect. 5 and Sect. 8 by using these initial data. However, a few examples are highly unstable and initial data with much greater precision are needed if one wishes to produce satisfactory numerical figures for their orbits. Our intention is to provide numerical data that are satisfactory for the purpose of action value calculations. Numerical data with higher precision can be found in [13].

On the tables of numerical data (Tables 1-16), $\mathcal{A}(x)$ is the numerical action value of the action-minimizing retrograde orbits, the symbol $\mathcal{A}_{\text{test}}$ stands for the action value of the test path (20) in Sect. 3, namely the upper bound for true action values of minimizers

Table 1. Initial data and action values for solutions in Fig. 4 ($\phi = \pi/4$)

(m_1, m_2)	Initial Position	Initial Velocity	$\mathcal{A}(x)$	$\mathcal{A}_{\text{test}}$	$\mathcal{A}_{\text{coll}}$
$(0.5, 0.5)*$	$(0.9013, 0.5831, -0.7422)$	$(-0.3098i, 1.4767i, -0.5834i)$	2.1833	2.1836	2.0269
$(1, 1)*$	$(0.7683, 0.3657, -1.1340)$	$(-0.6741i, 1.5652i, -0.8911i)$	5.4813	5.4835	5.3120
$(2, 2)$	$(0.6560, 0.1509, -1.6139)$	$(-1.0976i, 1.7320i, -1.2688i)$	14.7629	14.7690	14.9345
$(4, 4)$	$(0.5937, -0.0483, -2.1817)$	$(-1.5523i, 1.9812i, -1.7154i)$	42.3032	42.3052	44.1980
$(0.5, 8)$	$(0.8813, 0.2234, -2.2280)$	$(-3.1719i, 0.4170i, -1.7502i)$	14.2853	14.2861	14.7710
$(1, 8)$	$(0.8476, 0.1793, -2.2821)$	$(-3.0628i, 0.6070i, -1.7929i)$	23.3078	23.3108	24.2997
$(2, 8)$	$(0.7902, 0.1003, -2.3832)$	$(-2.8635i, 0.9499i, -1.8722i)$	40.4350	40.4530	42.4866
$(4, 8)$	$(0.7043, -0.0321, -2.5606)$	$(-2.5229i, 1.5130i, -2.0125i)$	71.8272	71.8428	76.0265

Table 2. Initial data and action values for solutions in Fig. 5 ($\phi = \pi/2$)

(m_1, m_2)	Initial Position	Initial Velocity	$\mathcal{A}(x)$	$\mathcal{A}_{\text{test}}$	$\mathcal{A}_{\text{coll}}$
$(0.8, 0.8)$	$(0.5986, 0.1924, -0.6328)$	$(-0.3905i, 1.6392i, -0.9990i)$	4.6800	4.6824	4.7357
$(0.6, 0.6)*$	$(0.6240, 0.2587, -0.5296)$	$(-0.2353i, 1.6294i, -0.8365i)$	3.3097	3.3108	3.2839
$(0.4, 0.4)*$	$(0.6634, 0.3448, -0.4033)$	$(-0.0238i, 1.6138i, -0.6360i)$	2.0661	2.0673	2.0048
$(0.2, 0.2)*$	$(0.7190, 0.4701, -0.2378)$	$(0.2751i, 1.5987i, -0.3748i)$	0.9562	0.9567	0.9074

Table 3. Initial data and action values for solutions in Fig. 6 ($\phi = \pi/2$)

(m_1, m_2)	Initial Position	Initial Velocity	$\mathcal{A}(x)$	$\mathcal{A}_{\text{test}}$	$\mathcal{A}_{\text{coll}}$
$(1, 7)$	$(0.7963, 0.0831, -1.3777)$	$(-2.6569i, 0.6893i, -2.1683i)$	22.5684	22.5853	23.4650
$(3, 7)$	$(0.6888, -0.0789, -1.5144)$	$(-2.2898i, 1.3229i, -2.3910i)$	50.2584	50.2830	53.0809
$(5, 7)$	$(0.6077, -0.2013, -1.6292)$	$(-2.0423i, 1.8266i, -2.5749i)$	74.8848	74.8949	79.6536
$(7, 7)$	$(0.5523, -0.3051, -1.7300)$	$(-1.8303i, 2.2211i, -2.7353i)$	97.2712	97.3335	104.019
$(1, 5)$	$(0.7449, 0.0956, -1.2227)$	$(-2.2097i, 0.8273i, -1.9269i)$	17.9843	17.9918	18.9882
$(3, 5)$	$(0.6177, -0.0931, -1.3875)$	$(-1.8298i, 1.5358i, -2.1895i)$	39.4550	39.4844	42.6424
$(5, 5)$	$(0.5315, -0.2280, -1.5179)$	$(-1.5863i, 2.0665i, -2.4007i)$	58.1129	58.1233	63.4343
$(1, 3)$	$(0.6782, 0.1148, -1.0225)$	$(-1.6030i, 1.0717i, -1.6121i)$	12.7300	12.7406	13.7021
$(3, 3)$	$(0.5249, -0.1148, -1.2302)$	$(-1.2207i, 1.8692i, -1.9454i)$	27.2922	27.2967	30.3876
$(1, 1)$	$(0.5792, 0.1403, -0.7195)$	$(-0.5204i, 1.6567i, -1.1363i)$	6.1754	6.1783	6.3521

in the inequality (21), and the symbol $\mathcal{A}_{\text{coll}}$ stands for the lower bound estimate for action values over collision paths obtained in (19).

There are certain cases which need to be handled with care. Theorem 1 is readily applied to cases where

$$\mathcal{A}(x) < \mathcal{A}_{\text{test}} < \mathcal{A}_{\text{coll}}.$$

Those which fail to fulfill requirements in Theorem 1 are marked by either * or $\diamond$. They correspond respectively to

$$(m_1, m_2)* : \quad \mathcal{A}_{\text{coll}} < \mathcal{A}(x) < \mathcal{A}_{\text{test}} \tag{41}$$

and

$$(m_1, m_2)\diamond : \quad \mathcal{A}(x) < \mathcal{A}_{\text{coll}} < \mathcal{A}_{\text{test}}. \tag{42}$$

In our examples there are 14 cases of (41), among them there are 10 cases whose existence follow from Theorem 2 instead of Theorem 1. For such cases we may replace $\mathcal{A}_{\text{coll}}$ by $\mathcal{A}^*_{\text{coll}}$, the lower bound estimates for action values of collision paths obtained in (27). From the first graph in Fig. 20 it is quite apparent that our examples with $m_1 = m_2$ are all covered by Theorem 2. We list the values of $\mathcal{A}^*_{\text{coll}}$ for these 10 cases in Table 17.

Table 4. Initial data and action values for solutions in Fig. 7 ($\phi = 2\pi/3$)

(m_1, m_2)	Initial Position	Initial Velocity	$\mathcal{A}(x)$	$\mathcal{A}_{\text{test}}$	$\mathcal{A}_{\text{coll}}$
(0.2, 0.8)	(0.6865, 0.3135, −0.3881)	(−0.5258i, 1.1535i, −0.8176i)	2.5833	2.5867	2.5976
(0.4, 0.8)	(0.6281, 0.2348, −0.4391)	(−0.4306i, 1.3744i, −0.9273i)	3.4582	3.4628	3.5223
(0.6, 0.8)	(0.5817, 0.1696, −0.4847)	(−0.3613i, 1.5521i, −1.0249i)	4.2648	4.2704	4.3988
(0.8, 0.8)	(0.5434, 0.1139, −0.5259)	(−0.3093i, 1.7006i, −1.1130i)	5.0204	5.0256	5.2344
(0.2, 0.6)∗	(0.6741, 0.3309, −0.3334)	(−0.3076i, 1.2730i, −0.7023i)	2.1276	2.1311	2.1187
(0.4, 0.6)	(0.6111, 0.2429, −0.3902)	(−0.2076i, 1.5112i, −0.8237i)	2.8988	2.9047	2.9219
(0.6, 0.6)	(0.5607, 0.1729, −0.4401)	(−0.1468i, 1.6977i, −0.9305i)	3.6073	3.6120	3.6794
(0.2, 0.4)∗	(0.6554, 0.3485, −0.2705)	(−0.0292i, 1.4398i, −0.5701i)	1.6369	1.6394	1.6090
(0.4, 0.4)∗	(0.5867, 0.2501, −0.3347)	(0.0670i, 1.6989i, −0.7063i)	2.2982	2.3028	2.2867
(0.2, 0.2)∗	(0.6231, 0.3617, −0.1970)	(0.3719i, 1.7032i, −0.4150i)	1.0945	1.0961	1.0606

Table 5. Initial data and action values for solutions in Fig. 8 ($\phi = 2\pi/3$)

(m_1, m_2)	Initial Position	Initial Velocity	$\mathcal{A}(x)$	$\mathcal{A}_{\text{test}}$	$\mathcal{A}_{\text{coll}}$
(1, 7)	(0.8193, 0.0461, −1.1421)	(−2.5020i, 0.7013i, −2.4073)	23.1241	23.1600	23.8356
(3, 7)	(0.7026, −0.1211, −1.2602)	(−2.1812i, 1.3163i, −2.6706i)	49.1779	49.1903	51.4231
(5, 7)	(0.6259, −0.2529, −1.3595)	(−1.9253i, 1.7876i, −2.8867i)	72.2105	72.3221	76.1899
(7, 7)	(0.5644, −0.3579, −1.4456)	(−1.7419i, 2.1800i, −3.0670i)	93.2918	93.4163	98.9096
(1, 5)	(0.7528, 0.0523, −1.0141)	(−2.0771i, 0.8440i, −2.1428i)	18.4808	18.4997	19.2760
(3, 5)	(0.6231, −0.1428, −1.1556)	(−1.7254i, 1.5255i, −2.4516i)	38.7838	38.8214	41.3764
(5, 5)	(0.5364, −0.2829, −1.2674)	(−1.4950i, 2.0334i, −2.6918i)	56.4443	56.4514	60.8186
(1, 3)	(0.6686, 0.0602, −0.8492)	(−1.4832i, 1.0929i, −1.7955i)	13.1597	13.1775	14.1331
(3, 3)	(0.5140, −0.1716, −1.0268)	(−1.1400i, 1.8655i, −2.1764i)	27.1144	27.1280	30.1992
(1, 1)	(0.5334, 0.0653, −0.5987)	(−0.4353i, 1.7032i, −1.2679i)	6.5328	6.5436	6.9464

Table 6. Initial data and action values for solutions in Fig. 9 ($\phi = 3\pi/4$)

(m_1, m_2)	Initial Position	Initial Velocity	$\mathcal{A}(x)$	$\mathcal{A}_{\text{test}}$	$\mathcal{A}_{\text{coll}}$
(0.2, 0.8)	(0.6683, 0.2823, −0.3595)	(−0.4735i, 1.1856i, −0.8538i)	2.7193	2.7253	2.7567
(0.4, 0.8)	(0.6102, 0.2038, −0.4071)	(−0.3842i, 1.4050i, −0.9704i)	3.5998	3.6077	3.7073
(0.6, 0.8)	(0.5647, 0.1387, −0.4497)	(−0.3179i, 1.5808i, −1.0739i)	4.4136	4.4216	4.6084
(0.8, 0.8)	(0.5274, 0.0832, −0.4885)	(−0.2686i, 1.7273i, −1.1669i)	5.1730	5.1832	5.4677
(0.2, 0.6)	(0.6515, 0.2974, −0.3087)	(−0.2599i, 1.3092i, −0.7336i)	2.2416	2.2468	2.2506
(0.4, 0.6)	(0.5879, 0.2106, −0.3615)	(−0.1688i, 1.5491i, −0.8620i)	3.0265	3.0325	3.0810
(0.6, 0.6)	(0.5401, 0.1406, −0.4084)	(−0.1072i, 1.7318i, −0.9747i)	3.7445	3.7517	3.8644
(0.2, 0.4)∗	(0.6282, 0.3121, −0.2505)	(0.0157i, 1.4811i, −0.5956i)	1.7270	1.7306	1.7119
(0.4, 0.4)	(0.5601, 0.2154, −0.3102)	(0.1052i, 1.7422i, −0.7389i)	2.4074	2.4126	2.4186
(0.2, 0.2)∗	(0.5901, 0.3222, −0.1825)	(0.4133i, 1.7532i, −0.4333i)	1.1585	1.1614	1.1323

Table 7. Initial data and action values for solutions in Fig. 10 ($\phi = 3\pi/4$)

(m_1, m_2)	Initial Position	Initial Velocity	$\mathcal{A}(x)$	$\mathcal{A}_{\text{test}}$	$\mathcal{A}_{\text{coll}}$
(1, 7)	(0.8366, 0.0314, −1.0566)	(−2.4242i, 0.7065i, −2.5211i)	23.3797	23.3906	23.9582
(3, 7)	(0.7193, −0.1411, −1.1705)	(−2.1130i, 1.3068i, −2.8082i)	48.5301	48.5574	50.5045
(5, 7)	(0.6378, −0.2750, −1.2642)	(−1.8757i, 1.7738i, −3.0381i)	70.9024	70.9183	74.3437
(7, 7)	(0.5751, −0.3828, −1.3461)	(−1.6984i, 2.1598i, −3.2301i)	91.2663	91.3112	96.2175
(1, 5)	(0.7639, 0.0351, −0.9395)	(−2.0087i, 0.8507i, −2.2449i)	18.6978	18.7093	19.3712
(3, 5)	(0.6311, −0.1639, −1.0738)	(−1.6764i, 1.5214i, −2.5777i)	38.3957	38.4204	40.6749
(5, 5)	(0.5450, −0.3088, −1.1812)	(−1.4487i, 2.0154i, −2.8334i)	55.4811	55.5211	59.4243
(1, 3)	(0.6702, 0.0391, −0.7874)	(−1.4279i, 1.1037i, −1.8833i)	13.3502	13.3647	14.1970
(3, 3)	(0.5162, −0.1977, −0.9555)	(−1.0958i, 1.8597i, −2.2914i)	26.9694	26.9926	29.7414
(1, 1)	(0.5193, 0.0369, −0.5562)	(−0.3985i, 1.7280i, −1.3295i)	6.6987	6.7093	7.2245

Table 8. Initial data and action values for solutions in Fig. 11 ($\phi = 4\pi/5$)

(m_1, m_2)	Initial Position	Initial Velocity	$\mathcal{A}(x)$	$\mathcal{A}_{\text{test}}$	$\mathcal{A}_{\text{coll}}$
(0.2, 0.8)	(0.6596, 0.2659, −0.3447)	$(-0.4437i, 1.2046i, -0.8749i)$	2.7988	2.8064	2.8494
(0.4, 0.8)	(0.6019, 0.1873, −0.3906)	$(-0.3569i, 1.4232i, -0.9958i)$	3.6824	3.6923	3.8150
(0.6, 0.8)	(0.5567, 0.1224, −0.4320)	$(-0.2937i, 1.5984i, -1.1025i)$	4.4985	4.5097	4.7305
(0.8, 0.8)	(0.5199, 0.0670, −0.4695)	$(-0.2461i, 1.7444i, -1.1986i)$	5.2593	5.2748	5.6036
(0.2, 0.6)	(0.6401, 0.2799, −0.2959)	$(-0.2335i, 1.3308i, -0.7518i)$	2.3084	2.3144	2.3274
(0.4, 0.6)	(0.5780, 0.1932, −0.3471)	$(-0.1430i, 1.5691i, -0.8843i)$	3.0984	3.1071	3.1737
(0.6, 0.6)	(0.5303, 0.1235, −0.3923)	$(-0.0846i, 1.7525i, -1.0007i)$	3.8225	3.8331	3.9721
(0.2, 0.4)∗	(0.6146, 0.2930, −0.2401)	$(0.0413i, 1.5056i, -0.6105i)$	1.7797	1.7840	1.7718
(0.4, 0.4)	(0.5472, 0.1971, −0.2977)	$(0.1273i, 1.7677i, -0.7580i)$	2.4695	2.4769	2.4953
(0.2, 0.2)∗	(0.5735, 0.3016, −0.1750)	$(0.4365i, 1.7828i, -0.4439i)$	1.1956	1.1995	1.1741

Table 9. Initial data and action values for solutions in Fig. 12 ($\phi = 4\pi/5$)

(m_1, m_2)	Initial Position	Initial Velocity	$\mathcal{A}(x)$	$\mathcal{A}_{\text{test}}$	$\mathcal{A}_{\text{coll}}$
(1, 7)	(0.8522, 0.0231, −1.0141)	$(-2.3680i, 0.7080i, -2.5878i)$	23.4679	23.5160	24.0139
(3, 7)	(0.7315, −0.1527, −1.1255)	$(-2.0716i, 1.3007i, -2.8900i)$	48.0762	48.1552	49.9255
(5, 7)	(0.6477, −0.2887, −1.2178)	$(-1.8437i, 1.7637i, -3.1278i)$	69.9367	70.0436	73.1992
(7, 7)	(0.5847, −0.3994, −1.2971)	$(-1.6670i, 2.1427i, -3.3301i)$	89.9079	90.0063	94.5573
(1, 5)	(0.7752, 0.0253, −0.9016)	$(-1.9592i, 0.8529i, -2.3053i)$	18.7932	18.8251	19.4144
(3, 5)	(0.6384, −0.1766, −1.0323)	$(-1.6440i, 1.5175i, -2.6552i)$	38.1218	38.1621	40.2327
(5, 5)	(0.5518, −0.3241, −1.1383)	$(-1.4210i, 2.0049i, -2.9191i)$	54.8522	54.9375	58.5601
(1, 3)	(0.6750, 0.0273, −0.7569)	$(-1.3906i, 1.1083i, -1.9343i)$	13.4283	13.4702	14.2260
(3, 3)	(0.5195, −0.2126, −0.9206)	$(-1.0697i, 1.8559i, -2.3587i)$	26.8477	26.8987	29.4530
(1, 1)	(0.5133, 0.0214, −0.5347)	$(-0.3763i, 1.7429i, -1.3666i)$	6.7864	6.8050	7.3865

Table 10. Initial data and action values for solutions in Fig. 13 ($\phi = 4\pi/5$)

(m_1, m_2)	Initial Position	Initial Velocity	$\mathcal{A}(x)$	$\mathcal{A}_{\text{test}}$	$\mathcal{A}_{\text{coll}}$
(0.01, 4)	(0.8464, 0.1833, −0.7417)	$(-1.9263i, 0.4705i, -1.8627i)$	6.5852	6.5915	6.5966
(0.1, 4)	(0.8334, 0.1669, −0.7508)	$(-1.9048i, 0.5208i, -1.8927i)$	7.5217	7.5311	7.5846
(0.5, 4)	(0.7816, 0.0998, −0.7899)	$(-1.8128i, 0.7291i, -2.0102i)$	11.5279	11.5464	11.8468
(0.8, 4)	(0.7460, 0.0550, −0.8170)	$(-1.7543i, 0.8726i, -2.0869i)$	14.3917	14.4082	14.9185
(0.01, 1)	(0.7389, 0.3361, −0.3435)	$(-0.7236i, 0.8704i, -0.8631i)$	2.2552	2.2570	2.2596
(0.1, 1)	(0.7072, 0.2944, −0.3652)	$(-0.6678i, 0.9894i, -0.9227i)$	2.7424	2.7487	2.7806
(0.5, 1)	(0.5994, 0.1492, −0.4489)	$(-0.4991i, 1.3968i, -1.1472i)$	4.6924	4.7027	4.9462
(0.8, 1)	(0.5438, 0.0677, −0.5028)	$(-0.4177i, 1.6184i, -1.2842i)$	5.9801	5.9982	6.4401

Table 11. Initial data and action values for solutions in Fig. 14 ($\phi = 4\pi/5$)

(m_1, m_2)	Initial Position	Initial Velocity	$\mathcal{A}(x)$	$\mathcal{A}_{\text{test}}$	$\mathcal{A}_{\text{coll}}$
(1, 100)	(1.93617, 0.00572, −2.50767)	(−7.06757, 0.13386, −6.31863)	137.950	138.0457	138.2022
(10, 100)	(1.82450, −0.15637, −2.60800)	(−6.70235, 0.73687, −6.66520)	821.639	822.4731	824.3510
(50, 100)	(1.48170, −0.71128, −2.95672)	(−5.46436, 2.80847, −7.62894)	3497.41	3499.1535	3511.6142
(100, 100)	(1.22396, −1.19099, −3.29748)	(−4.51049, 4.59515, −8.46580)	6305.41	6310.1779	6337.2166

For most of the cases we have numerical action values $\mathcal{A}(x)$ of true action minimizers which are fairly close to $\mathcal{A}_{\text{test}}$, and $\mathcal{A}_{\text{coll}}$ often stays well above action values of our test path. This suggests that action-minimizers tend to be Keplerian-like for both the pair m_1, m_1 and the pair m_3, $m_1 + m_2$. Among the examples we have, there are 3 cases of type (42), for which the relative motions of m_1 and m_2 are less like Keplerian orbits.

Table 12. Initial data and action values for solutions in Fig. 15 ($\phi = \pi$)

(m_1, m_2)	Initial Position	Initial Velocity	$\mathcal{A}(x)$	$\mathcal{A}_{\text{test}}$	$\mathcal{A}_{\text{coll}}$
(0.2, 0.8)	(0.6387, 0.2122, −0.2975)	$(-0.3249i, 1.2793i, -0.9584i)$	3.1012	3.1226	3.2024
(0.4, 0.8)	(0.5822, 0.1326, −0.3390)	$(-0.2495i, 1.4969i, -1.0977i)$	3.9938	4.0224	4.2254
(0.6, 0.8)	(0.5382, 0.0673, −0.3768)	$(-0.1966i, 1.6709i, -1.2188i)$	4.8164	4.8525	5.1956
(0.8, 0.8)	(0.5016, 0.0115, −0.4104)	$(-0.1571i, 1.8181i, -1.3288i)$	5.5925	5.6305	6.1211
(0.2, 0.6)	(0.6116, 0.2231, −0.2562)	$(-0.1277i, 1.4129i, -0.8222i)$	2.5582	2.5776	2.6199
(0.4, 0.6)	(0.5511, 0.1362, −0.3021)	$(-0.0484i, 1.6529i, -0.9724i)$	3.3703	3.3978	3.5267
(0.6, 0.6)	(0.5043, 0.0663, −0.3423)	$(0.0020i, 1.8395i, -1.1049i)$	4.1201	4.1501	4.3824
(0.2, 0.4)	(0.5758, 0.2323, −0.2081)	$(0.1322i, 1.6018i, -0.6672i)$	1.9766	1.9912	1.9999
(0.4, 0.4)	(0.5112, 0.1369, −0.2592)	$(0.2109i, 1.8702i, -0.8324i)$	2.7047	2.7266	2.7878
(0.2, 0.2)∗	(0.5231, 0.2354, −0.1517)	$(0.5179i, 1.9034i, -0.4843i)$	1.3372	1.3473	1.3331

Table 13. Initial data and action values for solutions in Fig. 16 ($\phi = \pi$)

(m_1, m_2)	Initial Position	Initial Velocity	$\mathcal{A}(x)$	$\mathcal{A}_{\text{test}}$	$\mathcal{A}_{\text{coll}}$
(1, 7)	(0.9220, −0.0068, −0.8741)	$(-2.1389i, 0.7162i, -2.8744i)$	23.8531	24.0013	24.1111
(3, 7)	(0.7913, −0.1990, −0.9812)	$(-1.9004i, 1.2788i, -3.2504i)$	46.2670	46.4415	47.3987
(5, 7)	(0.7009, −0.3474, −1.0727)	$(-1.7008i, 1.7190i, -3.5293i)$	66.1712	66.3543	68.3333
(7, 7)	(0.6328, −0.4683, −1.1520)	$(-1.5428i, 2.0802i, -3.7615i)$	84.3250	84.5245	87.5574
(1, 5)	(0.8267, −0.0096, −0.7789)	$(-1.7628i, 0.8653i, -2.5638i)$	19.1647	19.2727	19.4900
(3, 5)	(0.6825, −0.2282, −0.9062)	$(-1.5003i, 1.4969i, -2.9836i)$	36.9147	37.0432	38.3030
(5, 5)	(0.5892, −0.3875, −1.0086)	$(-1.3056i, 1.9644i, -3.2936i)$	52.3279	52.4590	54.8854
(1, 3)	(0.7032, −0.0157, −0.6561)	$(-1.2328i, 1.1296i, -2.1559i)$	13.7845	13.8756	14.2767
(3, 3)	(0.5415, −0.2703, −0.8137)	$(-0.9641i, 1.8481i, -2.6519i)$	26.3570	26.4648	28.1940
(1, 1)	(0.5015, −0.0330, −0.4686)	$(-0.2861i, 1.8041i, -1.5180i)$	7.1300	7.1751	8.0032

Table 14. Initial data and action values for solutions in figure 17 ($\phi = \pi$)

(m_1, m_2)	Initial Position	Initial Velocity	$\mathcal{A}(x)$	$\mathcal{A}_{\text{test}}$	$\mathcal{A}_{\text{coll}}$
(0.01, 4)⋄	(0.8967, 0.1574, −0.6386)	$(-1.6680i, 0.5064i, -2.0088i)$	7.6246	7.6281	7.6266
(0.1, 4)⋄	(0.8833, 0.1396, −0.6468)	$(-1.6576i, 0.5546i, -2.0526i)$	8.4913	8.5276	8.5214
(0.5, 4)	(0.8272, 0.0670, −0.6816)	$(-1.6039i, 0.7542i, -2.2150i)$	12.2146	12.3038	12.3835
(0.8, 4)	(0.7917, 0.0183, −0.7065)	$(-1.5567i, 0.8902i, -2.3154i)$	14.8662	14.9676	15.1680
(0.01, 1)	(0.7274, 0.2887, −0.2960)	$(-0.5776i, 0.9366i, -0.9308i)$	2.6077	2.6114	2.6155
(0.1, 1)	(0.6940, 0.2451, −0.3145)	$(-0.5304i, 1.0571i, -1.0040i)$	3.0955	3.1115	3.1627
(0.5, 1)	(0.5871, 0.0966, −0.3902)	$(-0.3866i, 1.4605i, -1.2672i)$	5.0356	5.0710	5.4377
(0.8, 1)	(0.5318, 0.0139, −0.4394)	$(-0.3200i, 1.6803i, -1.4243i)$	6.3229	6.3670	7.0081

Table 15. Initial data and action values for solutions in Fig. 18 ($\phi = \pi$)

(m_1, m_2)	Initial Position	Initial Velocity	$\mathcal{A}(x)$	$\mathcal{A}_{\text{test}}$	$\mathcal{A}_{\text{coll}}$
(10, 100)⋄	(2.0561, −0.1833, −2.2351)	(−6.26188, 0.7013, −7.5127)	746.294	747.3566	747.0770
(50, 100)	(1.6666, −0.8074, −2.5932)	(−5.13402, 2.6533, −8.6320)	3121.82	3122.6917	3129.5061
(100, 100)	(1.3752, −1.3459, −2.9376)	(−4.24437, 4.3405, −9.6090)	5616.38	5617.1174	5634.9039

Even though Theorem 1 does not apply to these cases, one can still choose test paths carefully so that their action values are between $\mathcal{A}(x)$ and $\mathcal{A}_{\text{coll}}$. In other words, we can still establish existence of these orbits by selecting test paths that are sufficiently close to true action-minimizers and by making use of (19).

Similar to the cases of retrograde orbits, on Table 18 of numerical data for prograde orbits displayed in Figure 21, $\mathcal{A}(x)$ represents numerical action values of orbits obtained in Theorem 3, $\mathcal{A}_{\text{test}}$ denotes action values of the test path (31) given by the lower bound

Table 16. Initial data and action values for solutions in Fig. 19 ($\phi = 5\pi/4$)

(m_1, m_2)	Initial Position	Initial Velocity	$\mathcal{A}(x)$	$\mathcal{A}_{\text{test}}$	$\mathcal{A}_{\text{coll}}$
(0.5, 0.5)	(0.4918, 0.0426, −0.2672)	(0.2015, 1.9829, −1.0922)	3.7236	3.8157	3.9768
(1, 1)	(0.5089, −0.0918, −0.4170)	(−0.1628, 1.8973, −1.7345)	7.5066	7.7055	7.9717
(2, 2)	(0.5533, −0.2491, −0.6083)	(−0.5640, 1.8414, −2.5549)	15.9065	16.2605	16.5537
(4, 4)	(0.6338, −0.4240, −0.8392)	(−0.9910, 1.8774, −3.5457)	36.5253	37.1206	37.4317

Table 17. Cases of type (41) with $m = m_1 = m_2$ from Tables 1-12. Here $\mathcal{A}^*_{\text{coll}}$ represents the lower bound in (27)

(m, ϕ)	$(0.5, \pi/4)$	$(1, \pi/4)$	$(0.2, \pi/2)$	$(0.4, \pi/2)$	$(0.6, \pi/2)$
$\mathcal{A}^*_{\text{coll}}$	2.6222	7.3923	1.0147	2.3994	4.1143
(m, ϕ)	$(0.2, 2\pi/3)$	$(0.4, 2\pi/3)$	$(0.2, 3\pi/4)$	$(0.2, 4\pi/5)$	$(0.2, \pi)$
$\mathcal{A}^*_{\text{coll}}$	1.1679	2.6813	1.2396	1.2813	1.4404

Table 18. Initial data and action values for prograde solutions in Fig. 21

(m, η)	Initial Position	Initial Velocity	$\mathcal{A}(x)$	$\mathcal{A}_{\text{test}}$	$\mathcal{A}_{\text{coll}}$
(1.5, 1.25)	(0.27877, 0.04165, −0.48063)	(2.62717i, −1.44573i, −1.77216i)	18.0564	18.1397	18.5481
(2, 1.25)	(0.27456, 0.00280, −0.55471)	(2.66332i, −1.64288i, −2.04088i)	26.5282	26.6137	27.6994
(1, 1)	(0.34357, 0.10696, −0.45053)	(2.30073i, −0.93097i, −1.36976i)	9.7838	9.8075	10.0834
(1.5, 1)	(0.32849, 0.04507, −0.56035)	(2.33063i, −1.20013i, −1.69575i)	16.5371	16.5716	17.5727
(2, 1)	(0.32038, 0.00197, −0.64470)	(2.38571i, −1.40988i, −1.95166i)	24.4253	24.4555	26.4922
(0.5, 0.5)	(0.59029, 0.34678, −0.46853)	(1.77698i, −0.31495i, −0.73102i)	3.0921	3.0955	3.2175
(1, 0.5)	(0.51250, 0.20293, −0.71543)	(1.85867i, −0.74190i, −1.11677i)	7.5222	7.5254	8.4324
(1.5, 0.5)	(0.47412, 0.11700, −0.88667)	(1.93521i, −1.01320i, −1.38302i)	13.0854	13.0924	15.3226
(2, 0.5)	(0.45209, 0.05747, −1.01911)	(2.01149i, −1.21673i, −1.58952i)	19.6905	19.6961	23.7071
(0.5, 0.25)	(0.87638, 0.60624, −0.74131)	(1.54970i, −0.38575i, −0.58198i)	2.3955	2.3961	2.6222
(1, 0.25)	(0.73855, 0.39467, −1.13322)	(1.64887i, −0.76113i, −0.88774i)	6.1544	6.1587	7.3923
(1.5, 0.25)	(0.66528, 0.27024, −1.40328)	(1.74023i, −1.00711i, −1.09968i)	11.0275	11.0366	13.9051
(2, 0.25)	(0.62206, 0.18484, −1.61379)	(1.81864i, −1.18703i, −1.26322i)	16.8920	16.9142	21.9526

in (21), and $\mathcal{A}_{\text{coll}}$ stands for the lower bound estimates for action values of collision paths obtained in (30). We list initial data to the fifth decimal place because of the instability of many action-minimizing prograde orbits.

Acknowledgement. This research work is partly supported by the National Science Council and the National Center for Theoretical Sciences in Taiwan.

References

1. Barutello, V., Ferrario, D., Terracini, S.: Symmetry groups of the planar three-body problem and action-minimizing trajectories. Arch. Ration. Mech. Anal. **190**, 189–226 (2008)
2. Broucke, R.: On relative periodic solutions of the planar general three-body problem. Celes. Mech. **12**, 439–462 (1975)
3. Chen, K.-C.: Binary decompositions for the planar N-body problem and symmetric periodic solutions. Arch. Ration. Mech. Anal. **170**, 247–276 (2003)
4. Chen, K.-C.: Removing collision singularities from action minimizers for the N-body problem with free boundaries. Arch. Ration. Mech. Anal. **181**, 311–331 (2006)
5. Chen, K.-C.: Existence and minimizing properties of retrograde orbits to the three-body problem with various choices of masses. Annals of Math. **167**, 325–348 (2008)
6. Chen, K.-C.: *Variational constructions for some satellite orbits in periodic gravitational force fields.* Amer. J. Math. (2009, to appear)

7. Chenciner, A.: *Symmetries and "Simple" Solutions of the Classical N-body Problem*. Proceeding of ICMP, Lisbone, 2003, River Edge, NJ, World Scientific, 2006
8. Chenciner, A., Féjoz, J., Montgomery, R.: Rotating eights I. Nonlinearity **18**, 1407–1424 (2005)
9. Chenciner, A., Montgomery, R.: A remarkable periodic solution of the three-body problem in the case of equal masses. Ann. Math. **152**, 881–901 (2000)
10. Ferrario, D., Terracini, S.: On the existence of collisionless equivariant minimizers for the classical n-body problem. Invent. Math. **155**, 305–362 (2004)
11. Gordon, W.: A minimizing property of Keplerian orbits. Amer. J. Math. **99**, 961–971 (1977)
12. Hénon, M.: A family of periodic solutions of the planar three-body problem, and their stability. Celes. Mech. **13**, 267–285 (1976)
13. http://www.math.nthu.edu.tw/~kchen/retrograde.html
14. Meyer, K.R.: *Periodic Solutions of the N-body Problem*. Lecture Notes in Mathematics, Vol. **1719**, Berlin: Springer-Verlag, 1999
15. Marchal, C.: *The Three-Body Problem*. Studies in Astronautics, **4**. Amsterdam: Elsevier Science Publishers, B.V., 1990
16. Moeckel, R.: A topological existence proof for the Schubart orbits in the collinear three-body problem. Discrete Contin. Dyn. Syst. Ser. B **10**, 609–620 (2008)
17. Montgomery, R.: The N-body problem, the braid group, and action-minimizing periodic solutions. Nonlinearity **11**, 363–376 (1998)
18. Moore C.: Braids in classical dynamics. Phy. Rev. Lett. **70**, 3675–3679 (1993)
19. Palais, R.: The principle of symmetric criticality. Commun. Math. Phys. **69**, 19–30 (1979)
20. Schubart, J.: Numerische Aufsuchung periodischer Lösungen im Dreikörperproblem. Astr. Nachr. **283**, 17–22 (1956)
21. Simó, C.: *Choreographic solutions of the planar three body problem*. http://www.maia.ub.es/dsg/3body.html
22. Szebehely, V.: *Theory of Orbits – The Restricted Problem of Three Bodies*. New York: Academic Press, 1967
23. Venturelli, A.: A variational proof of the existence of von Schubart's orbit. Discrete Contin. Dyn. Syst. Ser. B **10**, 699–717 (2008)

Communicated by G. Gallavotti